Master's thesis

NTNU
Norwegian University of Science and Technology
Faculty of Information Technology and Electrical Engineering
Department of Electric Power Engineering

Marte Røine Brurås

Impact of Fast Charging Stations on the Reliability of Electricity Supply in Distribution Networks

Master's thesis in Energy and Environmental Engineering
Supervisor: Gerd Kjølle
June 2019

NTNU
Norwegian University of Science and Technology

Marte Røine Brurås

Impact of Fast Charging Stations on the Reliability of Electricity Supply in Distribution Networks

Master's thesis in Energy and Environmental Engineering
Supervisor: Gerd Kjølle
June 2019

Norwegian University of Science and Technology
Faculty of Information Technology and Electrical Engineering
Department of Electric Power Engineering

NTNU
Norwegian University of
Science and Technology

Problem description

The electrification of the Norwegian transport sector leads to an increasing need for fast charging of electric vehicles (EVs) and electric road freight transport in the following years. Thus, it is predicted that there will be a massive increase in the number of fast charging stations along Norwegian main roads in the near future. This could cause several challenges for the existing power system.

In this master thesis will the impact of a fast charging station on the reliability of electricity supply be investigated for an existing distribution grid operated by Skagerak Nett. The reliability analyzes will examine future scenarios towards 2050, where different locations for the fast charging station will be in focus.

The master thesis includes the following studies:

- Finding an optimal location for a fast charging station on the basis of minimizing reliability indices
- Reliability analyzes of the day with estimated maximum power demand at the fast charging station with the optimal location

Preface

This master thesis is submitted at the Department of Electric Power Engineering at the Norwegian University of Science and Technology (NTNU) in Trondheim.

I would first and foremost like to thank my supervisor, Gerd Hovin Kjølle, for valuable help and guidance throughout this process. Hanne Vefsnmo has been an important resource for me in order to perform analyzes using the FASaD prototype, and I am grateful for your help. The master thesis could additionally not be conducted without the extensive power system data provided by Skagerak Nett.

I would also like to thank all my family, friends and boyfriend for motivation and encouragement during this process.

Marte Røine Brurås, Trondheim, 05.06.2019

Abstract

By 2050, Norway has an ambition of becoming a low-carbon country with a zero-emission transport sector. This leads to a massive increase in electrified transport and the following need for charging. Thus, fast charging stations with significantly high power demands are currently being installed across Norway.

This master thesis investigates the impact a fast charging station will have on the reliability of electricity supply in a power grid. Reliability analyzes by the simulation tool named the FASaD prototype is conducted for an existing distribution grid operated by Skagerak Nett. A fast charging station with a power demand of 10 MW is included in the simulations. Different locations for the fast charging station near the main road in Sande municipality are explored, in order to find an optimal location that minimizes the impact on the reliability of supply. Further, a reliability analysis of the 'worst-case' scenario is performed. June 29 is chosen to be the 'worst-case' scenario, as it is assumed that the maximum power demand for the fast charging station will occur on this day.

The results of the reliability analyzes show that the location for the fast charging station, relative to the transformer and the reserve connections, will have an impact on the reliability of supply. It is found that the most optimal location in the examined grid is a substation located some distance downstream from the transformer and very close to a reserve connection. From the simulations, it is found that the different locations lead to changes in the switching sequences during a fault, which impacts the reliability of supply. All the examined alternative locations gave a massive increase in reliability indices. The increase was 176% for the annual interrupted power, while it was found a 236% - 258% increase in the annual cost of energy not supplied (CENS) and a 206% - 237% increase in the annual energy not supplied (ENS) for the different scenarios.

From analyzes of the 'worst-case' scenario, it was found that the variation in fault frequency

during a day had minimal impact on the reliability of supply. Further, it was found that total ENS and interrupted power for the investigated grid depended strongly on the load profile of the fast charging station. From hourly simulations using the FASaD prototype, minimal variation in the CENS during a day was found.

Sammendrag

Innen 2050 har Norge en ambisjon om å bli et lavutslippssamfunn med nullutslipp fra transportsektoren. Dette fører til en stor økning i elektrifisert transport, og følgende et behov for lading. Dermed installeres det i dag hurtigladestasjoner med høyt effektbehov i hele Norge.

Denne masteroppgaven undersøker hvilken påvirkning en hurtigladestasjon vil ha på leveringspåliteligheten i kraftnettet. Simuleringsverktøyet FASaD-prototypen er brukt til utføring av leveringspålitelighetsanalyser på et eksisterende distribusjonsnett driftet av Skagerak Nett. En hurtigladestasjon på 10 MW er inkludert i simuleringene. For å finne en optimal lokasjon som minimerer påvirkningen hurtigladestasjonen har på leveringspåliteligheten i nettet, er ulike lokasjoner nær hovedveien i Sande kommune undersøkt. Videre er det utført en analyse av et "worst-case" scenario. Det er funnet at 29. juni er "worst-case" scenario, ettersom det antas at det maksimale effektbehovet gjennom året for hurtigladestasjonen vil være på denne dagen.

Resultatene fra analysene viser at hurtigladestasjonenes plassering i forhold til transformator og reserveforbindelser vil påvirke leveringspåliteligheten i kraftnettet. Analysene viser at den mest optimale plasseringen i det undersøkte nettet er en hurtigladestasjon som er plassert et stykke ute i nettet og veldig nært en reservekobling. Fra simuleringene er det funnet at de ulike lokasjonene fører til endringer i brytersekvensene ved feil i nettet, noe som påvirker den totale leveringspåliteligheten. Alle de undersøkte alternative ga en stor økning i leveringspålitelighetsindekser. Det ble funnet en økning på 176 % for årlig avbrutt effekt, en 236 % - 258 % økning i årlig avbruddskostnader (KILE) og en økning på 206% - 237 % i årlig ikke levert energi (ILE).

Fra analyser av "worst-case"-scenarioet ble det funnet at variasjoner i feilfrekvensen i løpet av en dag har minimal påvirkning på leveringspåliteligheten i kraftnettet. Videre ble det

funnet at ILE og avbrutt effekt i løpet av en dag for et kraftnett var veldig avhengig av lastprofilen til hurtigladestasjonen. Fra simuleringer av hver time gjennom et døgn ved bruk av FASaD-prototypen ble det funnet minimal variasjon i KILE.

Abbreviations

ADT Average Daily Traffic.

BEV Battery Electric Vehicle.

CENS Cost of Energy Not Supplied.

DSO Distribution System Operator.

ENS Energy Not Supplied.

ENTSO-E European Network of Transmission System Operators for Electricity.

EV Electric Vehicle.

HEV Hybrid Electric Vehicle.

IEA International Energy Agency.

IEC International Electrotechnical Commission.

IRU The International Road Transport Union.

NTNU The Norwegian University of Science and Technology.

NVE The Norwegian Water Resources and Energy Directorate.

PHEV Plug-in Electric Vehicle.

PQ Power Quality.

SoC State of Charge.

TSO Transmission System Operator.

Contents

List of Figures

List of Tables

Chapter 1

Introduction

1.1 Motivation

The climate target set by the Norwegian government is ambitious. By 2030, the ambition is to be a climate neutral country, which involves a reduction of 40 % of the total emission compared to the reference year 1990. The long-term target for 2050 is to become a low-emission country, where the total emissions must be reduced by 80 to 95 % compared to 1990 [45]. The transport sector is currently responsible for a significant part of the domestic greenhouse gas emissions. The domestic road traffic is alone responsible for approximately 9 % of Norway's total emissions [34]. Thus, major cuts in this sector are necessary in order to reach the ambitious climate target. This has led to Governmental incentives for electrification of passenger vehicles, where the goal is to end the sale of new fossil fuel-power vehicles by 2025 [48]. Furthermore, it is predicted nearly a doubling in road freight transport on Norwegian road within the year 2050 [31]. To achieve the climate target must this sector also contribute to reducing emissions. Hence, a goal is determined, which involves that 50 % of all heavy-duty trucks and all new distribution vehicles should be zero-emission vehicles within 2030 [31].

In modern societies are a reliable supply of electricity crucial. The massive increase in electrified transport and the following need for fast charging stations can impact the reliability of supply in the power system. Particularly, the massive increase in power demand at one load point in the power grid, related to the installation of a fast charging station, could

cause significant challenges for the reliability of supply. Few studies have been carried out on this specific subject as the establishment of fast charging station across large parts of Norway is only in the beginning phase.

1.2 Purpose

The aim of this master thesis is to investigate the change in the reliability of supply in a power system due to the installation of fast charging stations. The analysis period will be towards 2050 in order to investigate the impact of an electrified road transport sector and the consequently required fast charging stations. A reliability calculation tool developed by SINTEF Energy Research is used to examine how different locations of a fast charging station will impact the reliability of supply of an existing grid in Sande municipality. The purpose is to find an optimal location in regards to minimizing specific annual reliability indices for the power system: the Cost of Energy Not Supplied (CENS), the interrupted power and Energy Not Supplied (ENS). Additionally, a reliability analysis of the day with the assumed maximum power demand at the fast charging stations during a year will be performed. The motive is to find out how the impact of a fast charging station on the reliability of supply changes during this day.

1.3 Outline of the master thesis

The master thesis will begin by presenting the most important theory that will be the basis for further analyzes. In chapter 2 will the Norwegian power system structure be briefly explained, while chapter 3 presents the essential aspects of reliability of electricity supply and the methods for calculation of the reliability of supply in a power system. Further will chapter 4 describe the current state and the prediction regarding electrification of the road transport sector. This chapter will focus on aspects of charging EVs and road freight transport at fast charging stations.

Chapter 5 presents the method that will be used for finding the impact a fast charging station will have on the reliability of supply in one of the power grids of Skagerak Nett. By using the reliability assessment tool named the FASaD prototype will primarily an optimal location for a fast charging station be found. Three scenarios with different locations for

the fast charging station will be investigated, and the aim is to find a location where reliability indices are minimal. Further, an analysis of the day with assumed peak demand at the fast charging station during the year will be carried out. In chapter 6 will all the results from the case study be presented and compared, while the results and sources of error will be discussed in chapter 7. Finally, chapter 8 will conclude the work done in this master thesis and chapter 8 will present suggestions for further work.

1.4 Limitations

To successfully connect a fast charging station to the existing distribution grid must many aspects be considered. This master thesis will only evaluate the impact a fast charging station will have on the reliability of supply of the system. However, an extra massive load in the power system due to the new fast charging station will additionally impact other parameters such as the voltage frequency, supply voltage and harmonics. Since the interest of this master thesis is to investigate the reliability of supply in the power system will the optimal location for the fast charging station only be decided based on a minimization of reliability indices. Additionally, a power-flow analysis has not been conducted, and the analyze is, therefore, not completely realistic.

A complete economic analysis will not be performed in this master thesis. However, the CENS will be calculated, and the decision of optimal location for the fast charging station will, among others, be taken based on this. Costs due to the development of the grid and the development of the fast charging station are not taken into consideration in the study.

Chapter 2

Power System structure

The Norwegian power system is divided into three grid levels: the transmission grid, the regional grid and the distribution grid. By EU legislation are both the regional and the distribution grid regarded as a distribution grid [40]. Figure 2.1 shows the three levels, where distribution grid has a voltage level up to 22 kV, the regional grid has a voltage level of 33 - 132 kV and the transmission grid have a voltage level of 132 kV, 300 kV and 420 kV.

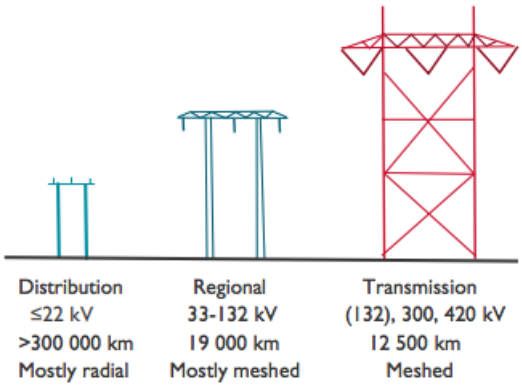

Figure 2.1: Grid levels [40]

The distribution grid, which is the grid analyzed in this master thesis, supplies power to smaller customers. This level is usually divided into one high-voltage and one low-voltage segment. The high-voltage segment is between 1 kV and 22 kV, while the low-voltage segment has a voltage level of 230V or 400 V [36].

Statkraft operates the transmission grid and is thereby called the Transmission System Operator (TSO), while the Distribution System Operators (DSOs) are operating the regional and distribution grids. The DSOs consist of approximately 130 different operators, with responsibility for major and minor areas across Norway [40].

From figure 2.1 can it be seen that the distribution grid consists of most radial grids, while regional and transmission grids mostly consist of meshed grids. In a radial grid are all components in series, which can be seen from the example of a radial grid in figure 2.2.

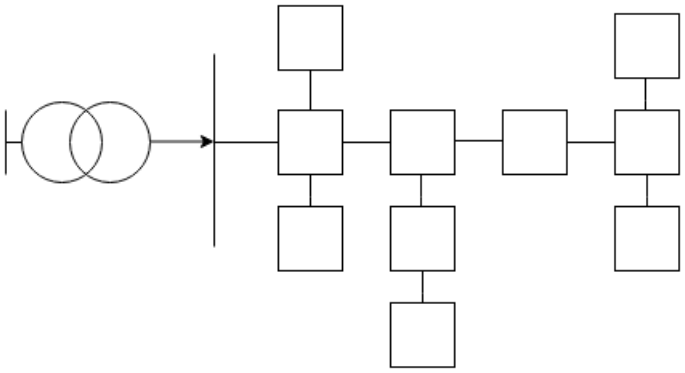

Figure 2.2: Radial grid

A radial grid usually consists of the main radial and several branches out from this radial. An alternative direction of the power flow is often eliminated due to the topography in the area. A considerable share of the grids outside the cities is developed as radial grids [12].

If a fault occurs in a radial grid will all customers located at the radial experience an interruption with duration equal to the time it takes to find and repair the fault. However, if a switch is placed on this radial will the customers upstream the switch have its power resupplied when the fault is located, while the customers downstream the switch will have a power outage until the fault is repaired [12].

In the cities in Norway will the distribution grid often consist of meshed grids. An example of a small meshed grid can be seen in figure 2.3. A meshed grid involves the possibility of high reliability of supply. Because of complicated and expensive grid protection in meshed grids are these grids usually operated as radial grids. The switches between some of the loads in figure 2.3 will be open during regular grid operation, and the mesh connections can thereby be considered as reserve connections during faults [12].

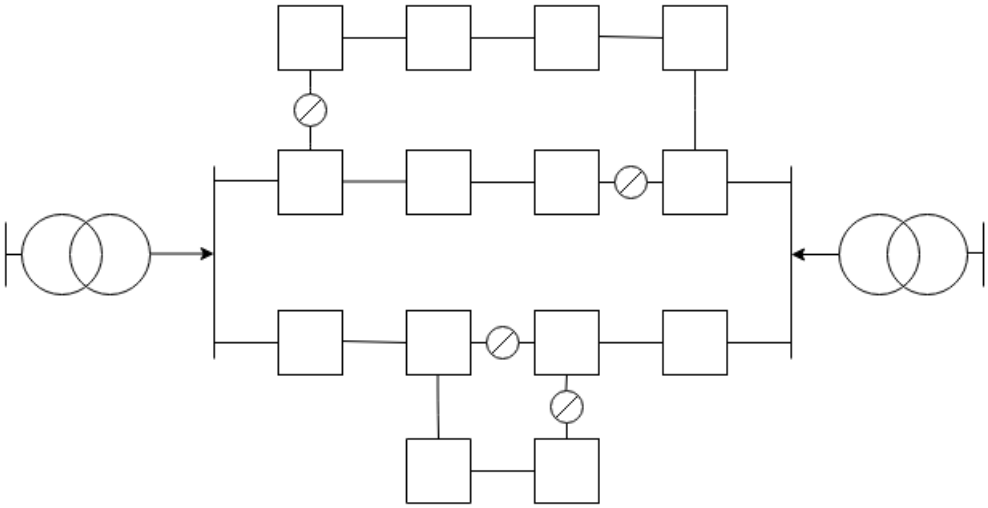

Figure 2.3: Meshed grid

The transformer, showed in both figure 2.2 and 2.3, is protected by a circuit breaker in situations of overcurrents or short circuits. This circuit breaker also protects the grid downstream from the transformer by blocking the current from flowing in the system during a fault.

Chapter 3

Reliability of electricity supply

The total performance of a power system can be defined by the collective term *quality of electricity supply*. This term includes four factors: the security of supply, power quality, reliability of supply and the customer relationship and pricing [25]. This master thesis will further mainly focus on the reliability aspect of the quality of electricity supply.

International Electrotechnical Commission (IEC) is defining the reliability of electricity supply as the following:

Reliability of electricity supply is the probability that an electric power system can perform a required function under given conditions for a given time interval[21].

The term is describing the availability of electrical energy in a power system [50]. More specifically, the analysis of reliability is a quantification of a power system's ability to distribute electricity to all customers in a power grid. Few interruptions over a significant period, and thereby a nearly continuous power supply, equals great reliability of electricity supply [21]. According to the report by an IEEE and CIGRE Task Force titled *Definition and Classification of Power System Stability*, reliability of supply can be determined by considering two aspects of the power grid [30]:

- **Adequacy** - A power system's ability to meet the electric power need of customers at all times.
- **Security** - A power system's ability to withstand rapid and unexpected disturbances in the system.

The stationary part of the power system is examined by an adequacy analysis, while a security analysis covers the dynamic part. This master thesis will primarily cover the adequacy aspect of the reliability analysis, as the stationary part of the system is the main focus of the analysis of this master thesis.

The requirements to ensure an acceptable reliability of supply is given in the Norwegian Power Quality (PQ) Code (*Forskrift om leveringskvalitet i kraftsystemet*) [44]. These regulations aim to achieve a quality of supply that will be beneficial for society in general. Hence, the costumer's rights will be well protected by the PQ Code [49]. The PQ Code imposes all power grid companies to register all interruptions that occur in the power system. The code requires the interruptions to be divided into short interruptions ($<$ 3 minutes) and long interruptions ($>$ 3 minutes) [44].

A supply interruption can be defined as a *condition in which the voltage at the supply terminals is lower than* 5% *of the reference voltage* [44]. Interruptions can be divided into two groups called prearranged and the accidental interruptions:

- **Prearranged** - When end-users are informed ahead of the interruptions, used to perform necessary work on the power grid
- **Accidental** - Sudden faults in the power system, either permanent or transient.

As the PQ Code requires, all interruption must be registered and classified correctly. The FASIT standard is a Norwegian standard used for this purpose [13]. This software is a platform for collection, calculation and reporting of reliability data [29]. Thus, all fault analysis performed by the grid companies are registered in the FASIT software, giving, among others, The Norwegian Water Resources and Energy Directorate (NVE) and Statnett a complete overview of the faults and interruptions in the power system. This registration makes the standardized measurement of reliability of supply possible.

The optimal socioeconomic level of reliability is given by minimization of five cost elements linked to the supply of electrical energy [1]. These are listed below:

- Investment costs
- Interruption costs

- Operation and Maintenance (O & M) costs
- Costs of electrical losses
- Bottleneck costs

The optimal socioeconomic level of reliability can be seen graphically in figure 3.1, where the minimization of the total cost gives the optimal level.

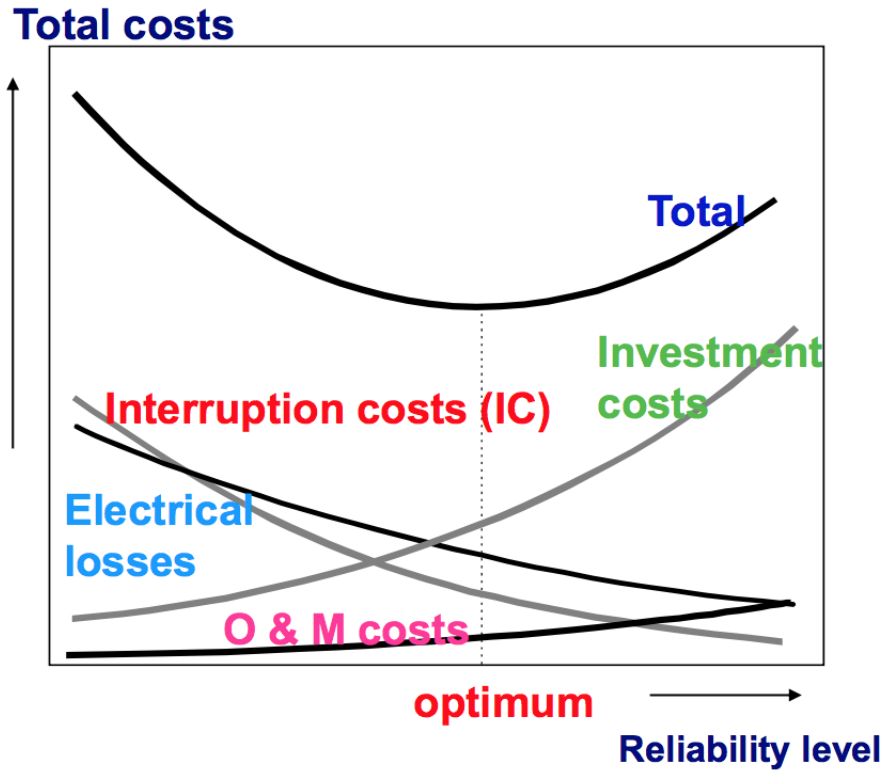

Figure 3.1: The socioeconomic optimal level of reliability [1]

A reliability level of almost 100% is theoretically reachable, but this will require enormous high investment costs [1]. The aim is, therefore, to find the optimal level of reliability that minimizes the total costs.

3.1 Faults in the power system

Supply interruptions are due to faults in the power system or maintenance causing planned disconnections. A fault is defined by IEC as *the state of an item characterized by inability to perform a required function* [22]. Faults are divided into two groups: permanent and transient. While permanent faults require corrective repair or maintenance, do transient faults only require reconnection of the circuit breaker. An interruption has previously been described as a period of time where the value of the supply voltage is less than 5% of the reference voltage.

Statnett collects statistics on all grid disturbances in the power system from the FASIT software, were all grid companies have registered the disturbances in their system [53]. In the period between 2009 and 2017, it has been registered an annual average of 10 224 grid disturbances in the Norwegian power system that have led to accidental interruptions, either long ($>$ 3 minutes) or short ($<$ 3 minutes) interruptions [53]. The surroundings are the leading cause of grid disturbances, and further causes the technical gear a great part of the total faults causing accidental interruptions. Additionally, a significant share of the grid disturbances has an unknown cause. The number of grid disturbances per hour will vary through the day, which is shown in figure 3.2.

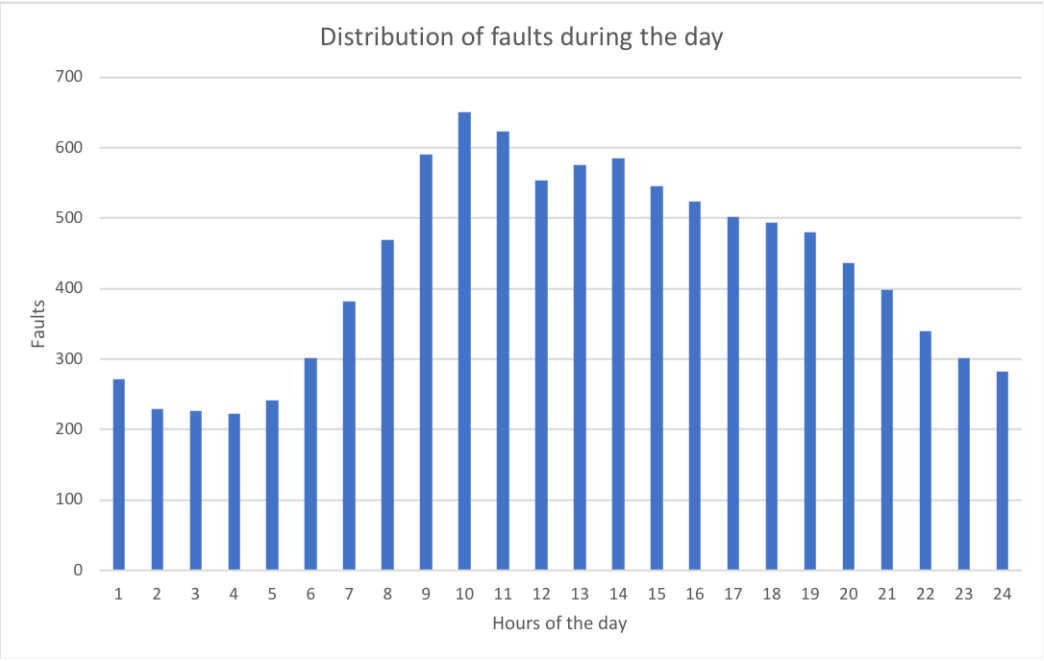

Figure 3.2: Distribution of grid disturbances during a day [53]

Figure 3.2 showed that the minimum number of faults occurs during the night, while there is a significant increase during the morning, with a maximum number of faults at 10 AM.

Statnett also gives an annual statistic on the fault frequency of different components in the power system. Components of particular interest are, among others, underground power cables and overhead lines. The annual average fault frequency of cables from the last ten year is 2.13 faults per 100 km/year, whereas for overhead lines is this fault frequency 7.05 faults per 100 km/year [53]. These fault frequencies represent both permanent and transient faults.

From the annual interruption statistics provided by NVE, from reliability data in FASIT, it can be seen that the reliability of supply in Norway is nearly stable and relatively high. On average is the availability of electricity to Norwegian end-users approximately 99,98 % [18]. The varying amount of faults due to extreme weather is one of the factors that will affect the availability. The NVE statistics shows e.g. a decrease in the reliability of supply to 99.965 % in 2011, which was mostly due to extreme weather causing faults in the system.

3.2 Reliability analyzes

Reliability analyzes are used to examine whether or not a power system meets the requirement of the reliability of supply given in the Norwegian PQ Code. Additionally, reliability analyzes are closely related to the end-users and the grid companies costs due to interruptions, as interruptions cost is an important outcome of these analyzes [1]. One of the main applications of reliability analyzes is to assess change in the reliability of supply due to changes in the power system. The current grid is compared with different scenarios to evaluate the best change and development of one specific grid [50].

Reliability analyzes are used as important tools for several projects within the power grid. [1] presents some of the most important outcomes of using reliability analyzes, which are among others:

- Power System Planning
- Design

- Assessment of development scenarios
- Establishment of reliability of supply standards
- Operation & Maintenance planning
- Contingency planning

Analysis methods for assessing the reliability of supply in a power system have been developed through many decades [26]. These analysis methods could be categorized into two main approaches: simulation methods and analytical methods. The simulation methods imply using Monte Carlo simulations, in which the actual system behaviour can be found. This is a time-consuming operation where small variations in the power system, such as different operating policies, can be modelled. Unlike the Monte Carlo simulation, analytic approaches are computationally effective. However, these methods have challenges with simulations of large and complex systems [26]. Both approaches are continually evolving and will provide more precise results for reliability calculations of real power systems. For the case study performed in this master thesis is an analytic approach for the calculation of the reliability of supply used.

Reliability analyzes will primarily calculate the main reliability indices, such as the expected number of annual interruptions and the time of these interruptions. Further can, among others, the annual ENS and annual CENS at each delivery point, as well as the annual interrupted power [50] be calculated. These values could also be found for smaller periods, e.g. values for each hour during one specific day.

3.3 Computations of reliability of electricity supply

3.3.1 Cost of Energy Not Supplied (CENS)

The Norwegian authorities, represented by NVE, regulates the network companies to secure an efficient operation of the power system. The economic revenue regulation is applied by, among others, an incentive scheme based on CENS. NVE describes CENS as *a measure of the calculated value of lost load for the customers*[39]. This measurement is an incentive for the network companies to perform sufficient maintenance of the grid components and

invest in new components when necessary, in order to reduce the CENS. Thus, the power outages will be reduced to the optimal socioeconomic level.

Reliability analyzes are used to estimate future CENS for different scenarios of investment and maintenance of the power system. The cost of all interruptions that are registered in FASIT, according to the Norwegian PQ Code, are included in the total CENS. This involves both short interruptions ($<$ 3 minutes) and long interruptions ($>$ 3 minutes) [28]. Additionally, the CENS is dependent on the duration of the interruption and the actual time the interruption occurs. Regularly updated cost functions are used to determine the actual cost of each individual interruption.

To accurately calculate the CENS are the customers divided into six groups. These are listed below [16]:

- Agriculture
- Residential
- Industry
- Commercial
- Public Sector
- Large industry

The CENS is required to be calculated for each interruption in a delivery point , due to regulations in FASIT [28]. Formula 3.1 estimates the cost of an interruption at any time j, from[16]:

$$C_j = c_{ref}(r) \cdot f_{Cj} \cdot \frac{P_{ref}}{P_j} \cdot P_j \tag{3.1}$$

where

C_j = Interruption cost for an interruption at time j (NOK)
$c_{ref}(r)$ = Cost rate in NOK/kW for duration r
f_{Cj} = Correction factor for cost (in monetary terms) at time j
P_{ref} = Interrupted power in kW at reference time
P_j = Interrupted power in kW at time j

$c_{ref}(r)$ is found from a cost function that varies for the different customer groups and for the length of the interruption. The regulations are presented in *Forskrift om økonomisk og teknisk rapportering, inntektsramme for nettvirksomheten og tariffer* by the Ministry of Petroleum and Energy [43].

The correction factor for cost f_Cj can more specifically be found by three factors, which is given in equation 3.2:

$$f_{Cj} = f_{Ch} \cdot f_{Cd} \cdot f_{Cm} \tag{3.2}$$

where

f_{Ch} = Correction factor for interruption cost (NOK) in hour h
f_{Cd} = Correction factor for interruption cost (NOK) in day d
f_{Cm} = Correction factor for interruption cost (NOK) in month m

The different correction factors will vary for the six customer groups, due to different predicted costs at different times. These correction factors can also be found in [43].

3.3.2 Interrupted Power and Energy Not Supplied (ENS)

Interrupted power and ENS are two important outcomes of reliability analyzes. Especially is ENS used to measure the reliability of a power system. In *Nordic and Baltic Grid Disturbance Statistics 2017*, European Network of Transmission System Operators for Electricity (ENTSO-E) summarizes the ENS in Norway in 2017. Grid disturbances in Norway caused this year a total ENS of $1113.7MWh$. Faults in overhead lines were the cause of 61% of the total ENS, whereas 29% of all faults were caused by faults in substations [10].

To define interrupted power will only accidental faults causing an interruption be taken into account. This is because reliability analyzes are based on the probability of a failure of a component. Whether or not an interruption occurs depends on the available capacity to deliver electricity to the load. [1]. Not sufficient capacity leads thereby to an interruption and disconnection of the load. Equations 3.3 and 3.4 explains when an interruption occurs [29]:

$$SAC + LC < P \tag{3.3}$$

or

$$APC < P \tag{3.4}$$

where

SAC = System Available Capacity [kWh/h]
LC = Local production at the delivery point [kWh/h]
APC = Available capacity for a delivery point [kWh/h]
P = Load at the delivery point [kWh/h]

From this can the interrupted power be found 3.5, from [29]:

$$P_{interr,j} = P - SAC_j - LC \tag{3.5}$$

where

$P_{interr,j}$ = Interrupted power due to the outage j
SAC_j = System available capacity after the outage j

ENS is the calculated electrical energy that would have been delivered to the end-user if the interruption had not occurred [1]. Calculation of the ENS for an interruption can be executed by the following equation 3.6, from [47].

$$ENS_j = \int_{T1}^{T2} \Delta P(t) dt \tag{3.6}$$

where

ENS_j = Energy Not Supplied for interruption j
$T1$ = Time at the start of the interruption
$T2$ = Time when the energy supply is recovered
$\Delta P(t)$ = Average load

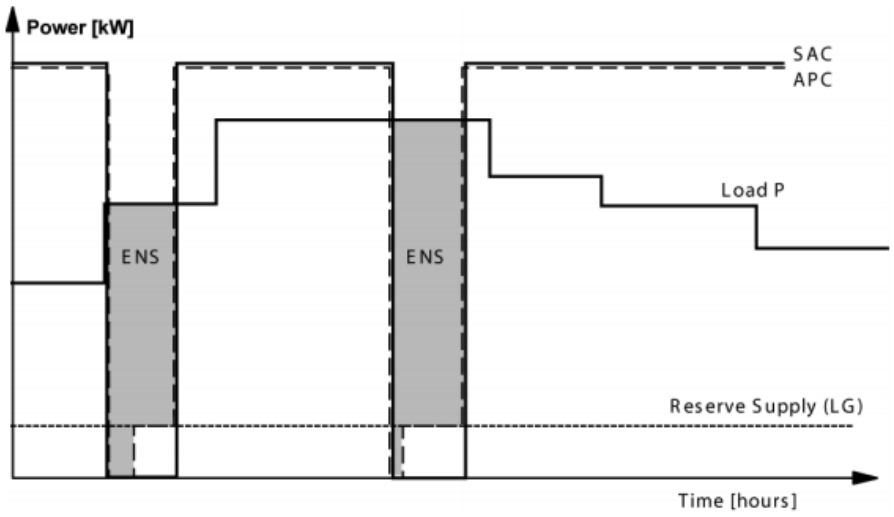

Figure 3.3: ENS in radial networks [29]

The ENS can be seen from the graphs in figure 3.3 as the area under the load profile where the APC (Available capacity for a delivery point) is less than the load. This example is from a radial network with a reserve supply (LG). It can be seen from this figure that a reserve supply will reduce the total ENS during an interruption.

3.3.3 Basic theory of reliability analysis

A well-known reliability analysis method used for quantitative estimations is the Markov model. With this model as the basis can simple formulas be developed to assess the reliability of a power system [1]. In a Markov process, there are two important terms [1]:

- Fault frequency (λ)
- Repair time (r)

Each component of the power system is included in this process, where the state of the components will be assessed. A component is assumed to either work as supposed to (state 1) or being repaired (state 0). This is illustrated in figure 3.4.

The function and repair cycle of a component in figure 3.4 shows how a component can

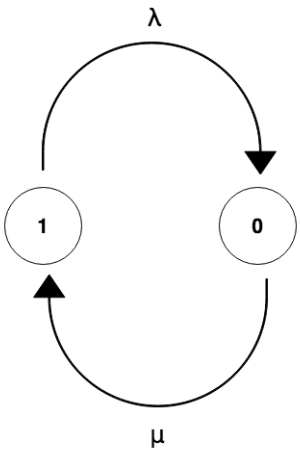

Figure 3.4: Function and repair cycle [1]

either be in state 0 or 1, while equations 3.7 and 3.8 explains how the parameters λ and μ can be found.

$$\lambda = \frac{1}{m} \tag{3.7}$$

$$\mu = \frac{1}{r} \tag{3.8}$$

where

μ = repair frequency
m = operating time

The repair time r is the time it takes to repair a permanent fault or the switching time during a temporary fault [1]. For components in series must all components be in state 1 for the system to function. For a system with components in parallel must only one of the components be in state 1 for the system to function.

3.3.4 The RELRAD model

The RELRAD model is an analytic approach that is used to estimate the reliability of supply in a power system. The model is developed by SINTEF Energy Research and The Norwegian University of Science and Technology (NTNU), and is used for the radial distribution system, as the name *RELiablity in a RADial network* implies [27]. Since all components in the radial power system are in series will a fault in one of the components cause the circuit breaker to trip, which would lead to interruptions for all delivery points in the grid [1]. Each component will represent a minimal cut, and the whole system will be a minimal cut set.

A minimal cut set is defined by [33] as

A minimal cut is a set of items that by failing secures that the system fails. A cut set is said to be minimal if it cannot be reduced without losing its status as a path set.

Figure 3.5 demonstrates the minimal cut set for the load point L_1. A failure in one of the components between the supply point and the load point will give interruption to the load point.

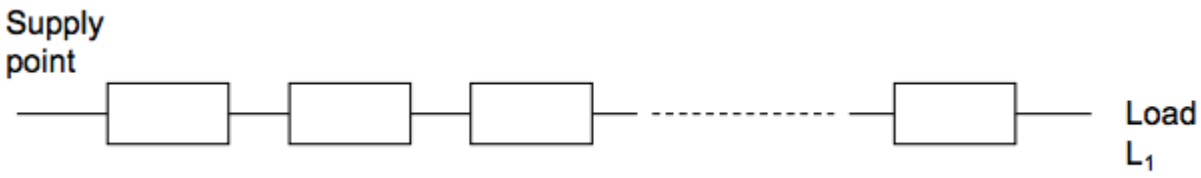

Figure 3.5: Minimal cut set [27]

The RELRAD model is based on the fault contribution from every component in the power grid. If it occurs a fault at one of the grid components can this model detect, by the topology and switch functions, which load points that will experience an interruption. Additionally, the duration of the interruption for a load point can be found.

The duration of interruption at specific load points will, among others, depend on the locations of the circuit breakers. Some load points will have the supply restored shortly after the fault occurred, where the duration of the interruption is only dependent on the sectioning time. Different load points will have an interruption until the fault is repaired [27]. The repair time is defined as the time from the beginning of the repair until the

correct function of the component is restored. Further is the sectioning time defined as the time between the fault is noticed and the fault is isolated between the switches closest to the fault location [1].

Each components' contributions to the duration and frequency of interruptions for load points are registered, which can be seen in figure 3.6 below. The contribution of different components to the respective reliability indices is thereby collected. Thus, the total sum of reliability indices for the whole power system can easily be found.

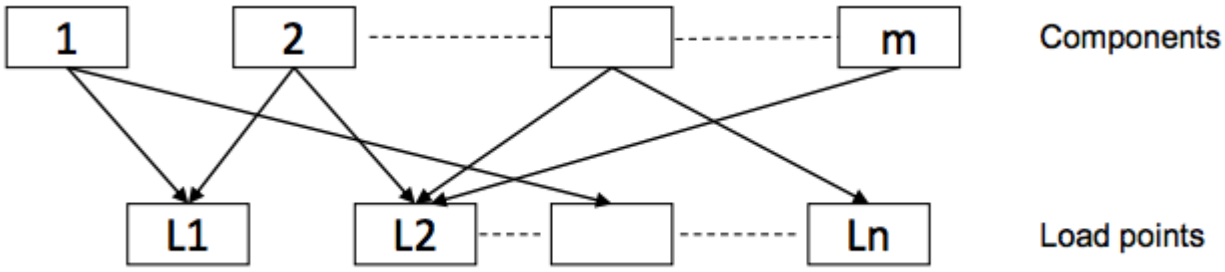

Figure 3.6: RELRAD approach [27]

By observing figure 3.6 it can, for instance, be seen that a fault in component number 2 will cause interruptions for load points L1 and L2.

Assumptions for calculation by RELRAD model

Topological assumptions, given in [1] and [26]:

- Radial operation of the power system.
- A fault is isolated by the upstream circuit breaker. If there is a fault on this circuit breaker, the next upstream circuit breaker will isolate the fault.
- When the location of the fault is found will the upstream disconnector be opened and then the circuit breaker will be closed.

Statistical assumptions, given in [1] and [27]:

- All faults are statistically independent

- One fault is repaired before another fault occurs
- Multiple faults are not represented

Reliability indices

The calculation of reliability indices are presented in [1] and will be presented by the following equations. All indices are calculated as annual values.

The number of annual interruptions per year (λ), the annual duration of interruptions (U) and the average duration of interruptions (r) can be found by equations 3.9, 3.10 and 3.11 respectively.

$$\lambda = \sum_i \lambda_i \tag{3.9}$$

$$U = \sum_i \lambda_i r_i \tag{3.10}$$

$$r = \frac{U}{\lambda} = \frac{\sum_i \lambda_i r_i}{\sum_i \lambda_i} \tag{3.11}$$

where

i = Counter variable for the number of grid components
λ_i = Fault frequency for component i
r_i = Sum of repair time for component i and sectioning time

Further can the annual interrupted power and ENS be found by the following equations 3.12 and 3.13.

$$\Delta P_{interr} = P \cdot \sum_j \lambda_j \tag{3.12}$$

$$ENS = \sum_j ENS_j = P \cdot \sum_j \lambda_j \cdot r_j \tag{3.13}$$

where

ΔP_{interr} = Annual interrupted power at the delivery point
P = Average load during the year
λ_j = Fault frequency for component j
ENS_j = Contribution of ENS from component j

Finally, the expected annual CENS can be found by equation 3.14.

$$C = f_{C,P} \cdot P_{Ref} \sum_j \lambda_j C_{P,ref}(r_j) \tag{3.14}$$

P_{Ref} = Load at the reference time
$f_{C,P}$ = Correction factor for annual specific interruption cost
$C_{P,ref}$ = Specific interruption cost for the delivery point with duration r_j at the reference time

In this master thesis will a calculation tool named the FASaD prototype be used for reliability analysis. This method is based on the RELRAD model, and the reliability indices will be calculated as showed in the equations above. A closer explanation of this simulation tool can be found in chapter 5.

Chapter 4

Electrification of the road transport sector

The transport sector consists of four main groups: road transport, coastal transport, aviation and rail transport. This master thesis will focus on the road transport sector, which is responsible for 62% of the total energy consumption of transport in Norway [34]. Further, road transport could be grouped into among other passenger cars, vans, buses, trucks and long-distance transport/ trailers [38]. The fast charging station evaluated in the master thesis will supply power to passenger cars/vans and freight transport, which thereby will be the further area of focus.

4.1 Electric vehicles

4.1.1 Types of EVs

EV can be divided in three main groups: Hybrid Electric Vehicles (HEVs), Battery Electric Vehicles (BEVs) and Plug-in Electric Vehicles (PHEVs). PHEV have both an internal combustion engine and an electric motor that is being charged by an external power. HEV have the similar two motors, but the electric motor is charged by braking during the drive. In comparison, BEVs have only the electric motor which is charged primarily from an outlet [2]. This master thesis will exclusively focus on vehicles that are entirely electric,

thus will BEVs be the only vehicles that will be investigated. BEVs will from now on be referred to as EVs.

4.1.2 EV adoption

In the last decade, there has been a significant increase in the number of EVs in Norway. *The Nordic EV Outlook for 2018* by the International Energy Agency (IEA) presents the extensive development in the market share of EVs [42]. The development is shown in figure 4.1.

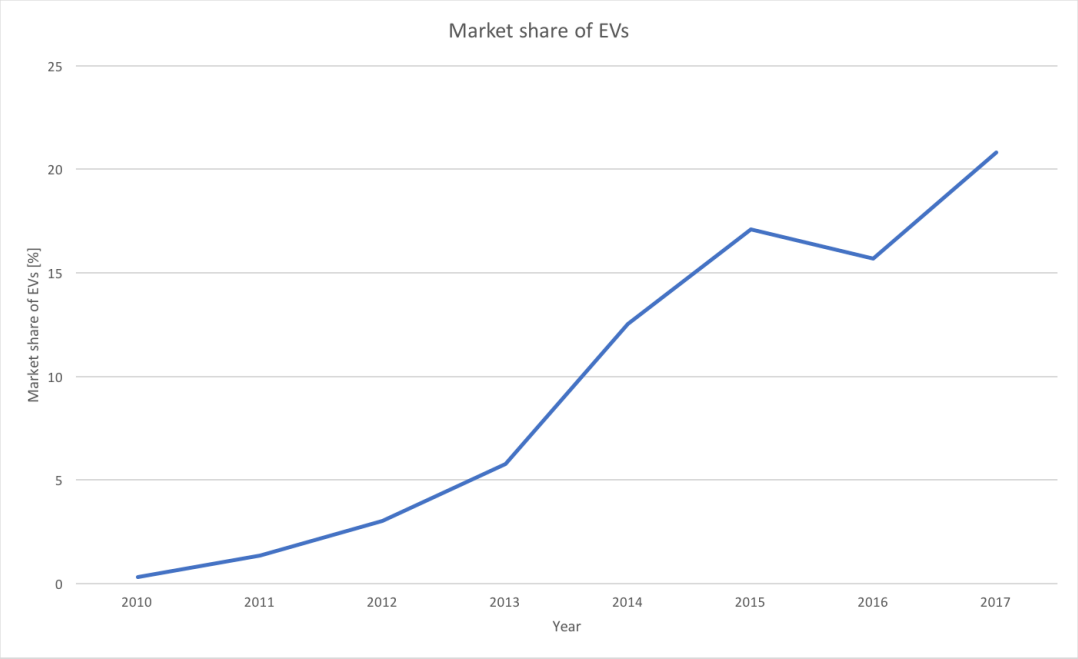

Figure 4.1: The market share of EVs in Norway[42]

From figure 4.1 it can be seen that a market share of 0.22% EVs in 2007 increased to 20.82% in 2017. According to the Norwegian Electric Vehicle Association (Elbilforeningen), approximately 200,000 EVs were on Norwegian roads by the end of 2018. This equals a vehicle share of 7.2% of the total passenger vehicle stock [4]. The most common vehicle types by the end of 2018 were Nissan Leaf and Volkswagen e-Golf, with respectively 25% and 16% of the total EVs [4]. Tesla is additionally a popular vehicle in Norway, where their Model S and Model X together have a share of approximately 15% of EVs in Norway. The capacity of these cars varies from Nissan Leaf at 24/30 kWh to Tesla at 100 kWh [4].

Increased range and capacity of EVs are expected in the following years, as the research and development of this sector are comprehensive.

As stated in [42], 70 % of the total Nordic stock of EVs is being located in Norway [42]. This is primarily a consequence of Norwegian EV policy where government incentives have achieved a high speed of the transition towards a fully electrified passenger vehicle fleet. The incentives include no purchase and import taxes, no annual road tax and no charges on ferries and roads. Currently, the present Government has determined to keep all the zero-emission incentives until the start of 2022. In the following years, all incentives will be revised and regulated according to the market development [4].

Conversion to full electrification of the transport sector is assumed to take several decades. Statistics Norway (Statistisk Sentralbyrå, SSB) assumes a population growth in Norway shown in table 4.1. A similar development is assumed by NVE for the growth in passenger vehicles [52], also presented in table 4.1.

	2014	**2030**	**2040**	**2050**
Population [mill]	5.1	5.9	6.3	6.6
All Passenger Vehicles [mill]	2.5	2.9	3.1	3.3

Table 4.1: Relationship between population growth and passenger vehicles [52]

NVE assumes that the ambition of the Norwegian Government to end the sale of new cars using fossil fuel by 2025 could lead to a continued rapid increase in EVs [51]. It is expected that the increase will be less steep near 2040 as a higher share of the population is assumed to be using public transport compared to today [52]. According to [51] will the Norwegian vehicle fleet consist of approximately 1.5 million EVs by 2030. An absolutely electrified passenger vehicle fleet could be reachable by 2040, or at least by the year 2050. From table 4.1 will this mean 3.3 millions EVs in Norway by 2050.

4.2 Road freight vehicles

It is predicted that in the future there will be a complete transfer to renewable energy in all of the transport sector. For freight transport using trucks and trailers could the fossil fuel that current is being used, be switched with mainly three types of renewable energy: biofuel, hydrogen and electricity[38]. With today's technology could some relatively light trucks

use an electric motor. The challenge is road freight transport that is particularly heavy or needs to have a wide range. Using the current battery technology in these vehicles will, in most cases, cause less efficient freight transport, and the use of hydrogen or biofuel might be more efficient solutions [38]. However, future electrification of road freight transport is by many considered as one of the most beneficial approaches for decarbonization of the transport sector [35]. The development of new and better technologies will possibly lead to new solutions, which today is challenging to predict.

4.2.1 Growth and electrification of road freight vehicles

The Norwegian Public Roads Administration (Statens Vegvesen) presents the expected growth in freight road transport on selected main roads across the southern parts of Norway. Their prognoses are a yearly growth in road freight transport of 2% [55]. Only vehicles with a length above 12.5 meters are included in these prognoses. In [55] are specific locations along the roads being analyzed, thus are measurable traffic data and future prognoses of the road E18 in Sande municipality available. This is of interest in this master thesis. The current and expected future number of road freight transport passing Bolstadtunellen in Sande is presented in tables 4.2 and 4.3.

Traffic Counting Station	**Road**	**Vehicles >12.5 m [ADT]**
Bolstad tunnel	E18	1625

Table 4.2: Today's ADT for road freight transport at Bolstad tunnel in Sande [55]

Traffic Counting Station	**Road**	**2030 [ADT]**	**2045 [ADT]**
Bolstad tunnel	E18	2102	2829

Table 4.3: Prognosis for future ADT for road freight transport at Bolstad tunnel in Sande [55]

In the tables is:

ADT = Average Daily Traffic (two-way passing vehicles)

From tables 4.2 and 4.3 it can be seen that the number of road freight vehicles passing Bolstad tunnel in 2045 is expected to be almost twice the number of 2018.

Nowadays, technologies for electrification of this sector is developing, with significant progress. As one of the leading manufacturers in Europe on commercial vehicles, MAN is making progress on the electrification of heavy-duty transport [11]. Since 2018 have MAN's e-truck been used on test operations and is expected to be used for transport from 2020. The e-trucks are expected to have a maximum range of 200 km with maximum batteries installed [17]. Additionally, the EV manufacturer Tesla is aiming to produce and deliver their first electrified truck in 2020, called Tesla Semi [54].

The International Road Transport Union (IRU) presents in 2017 the report *Commercial Vehicle of the Future* which addresses the ambition of fully sustainable truck operations [32]. The report concludes that in order to reach this goal must between 40% to 45% of the total road freight transport be electric by 2040 - 2050. Moreover, IRU predicts a common use of autonomous vehicles for road freight transport at this point in the future [32].

To increase the penetration of electric road freight transport must several challenges be overcome. This includes the challenges regarding the batteries, which today has limited range and the charging duration is long. Another critical challenge is the lack of public charging infrastructure [35].

4.3 Fast charging

Development within EV and charging technology leads to longer range and faster charging. Normal charging is applied by a Type 2 (AC) charger with a maximum power of 22 kW. Many municipalities have installed normal charging points, and these are currently available at many shopping centres and other similar places. However, fast chargers are being developed, and they are becoming common along parts of the Norwegian roads. Fast charging has several benefits, such as supporting roadside charging during long trips and thereby enable long-distance driving. Additionally, fast chargers provide energy quickly to EV owners who have forgotten to charge overnight or run empty during their trip [23].

A fast charger for EVs is a charger that is able to charge vehicles with an electric power of a minimum $22kW$. There exist today two fast charger standards, listed below [6]:

- **CHAdeMO**
- **Combo/CCS**

Both fast charging standards are DC charged with minimum 50 kW power.

Which of the two standards that are being used is dependent on the vehicle type. Some vehicle manufacturers have chosen to facilitate charging with the CHAdeMO charger and some with the CCS charger. Tesla has developed its own charging system, but their vehicles can charge by the regular standard chargers by, among others, using an adapter.

4.3.1 Fast charging of EVs

In 2017 was the average power achieved at the Norwegian fast charging stations 30.2 kW, while the average energy was 9.6 kWh. Further was the average charging time at fast charging stations 20.5 minutes [23]. This differs significantly from the nominal power of a minimum of 50 kW at fast chargers. Thus, the capacity of today's fast charging stations is not fully utilized.

Charging of EVs has been under development for several decades. The aim of faster charging with high capacity leads to significant development within this area. Today, fast chargers with a maximum power of 250 - 350 kW have entered the market. Electric vehicle manufacturer Tesla produces fast chargers, called Tesla Superchargers, with a peak power of 250 kW. These fast chargers are only available for Tesla models. Currently are the models S and X, which have 100 kWh batteries, able to charge with a power of 150 kW [8]. Thus, the capacity of the Supercharger is not yet fully utilized. IONITY, a joint venture between, among others, the BMW Group, Ford Motor Company and Volkswagen Group, opened the first fast charging station with a peak power of 350 kW in February 2019 in Denmark [3]. Further, IONITY will upgrade existing fast charging station to this power level [3]. Generally, the potential peak power at fast charging stations is higher than what today's vehicles can utilize. Institute of Transport Economics (Transportøkonomisk institutt) recommends that vehicle manufactures continues with research and development within battery technology so that EVs eventually can charge with the peak power at the fast charging stations [23]. This will cause a better user experience of EVs due to shorter charging time and better utilization of the battery [23].

With the future technological development of batteries could it be expected that the vehicles are able to utilize the power of the fast charging stations fully. Today's EVs have batteries with different technology and chemistry. Older EVs usually have a traditional low voltage lead-acid battery, while some other EVs have batteries based on sodium which

gives higher power and longer range. Many modern vehicles have lithium batteries. With lithium technology will the batteries have a high energy density, leading to high range [59]. Several vehicle producers such as Renault, Volkswagen and Nissan state that the future batteries in EVs will be solid-state batteries [9]. According to Renault is the aim to use these batteries within 2030. Many challenges must be overcome before this technology can be introduced to the market, but if it is successful will future batteries have significantly higher capacity and be charged with very high power [9]. Towards 2050, it is challenging to predict which technology that will be common for the use in EV, but it might, among others, be expected that the vehicles can charge with significantly higher power than today.

When charging the vehicle, the power will be limited by the vehicle itself. The charging power is dependent on the temperature of the battery and the State of Charge (SoC) [23]. SoC describes how full the battery is, and is measured in percentage compared to fully charged. Figure 4.2 presents the relationship between charging speed and SoC for different Nissan Leaf models. The relationship is found by Fastned, a Dutch development company for fast charging stations [14].

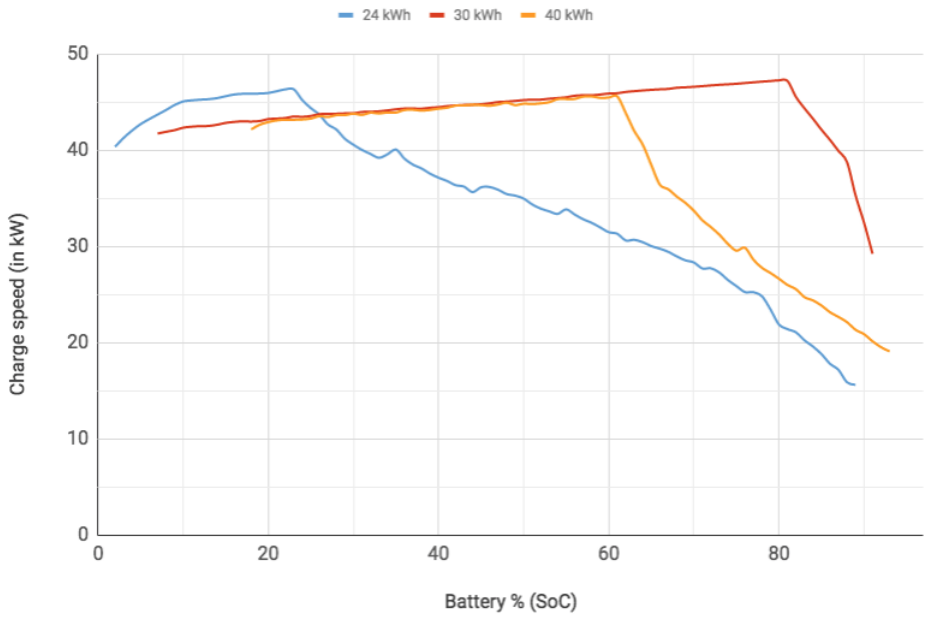

Figure 4.2: Charging speed of Nissan Leaf models [14]

It can be observed in figure 4.2 that the different Nissan Leaf models have different charging speeds. Nissan Leaf 30 kWh and Nissan Leaf 40 kWh have similar trends, where the charging speed is slightly increasing with the increase of SoC until the speed is suddenly

decreasing rapidly. Nissan 40 kWh entered the Norwegian market in 2018 and is today the only Nissan Leaf model available for purchasing, except for used car purchase. By inspection of the graph that represents this model, it is clear that the charging speed drops at a SoC of 60%. A significant share of EVs charged at charging stations are currently charged to a SoC of nearly 100% [6]. Therefore, Elbilforeningen recommends their members, in general, to charge their battery to a SoC of 80% to improve the efficiency of fast charging of multiple EVs in queue [6]. The EV charging power's dependence on temperature limits the charging speed in low ambient temperatures [23]. In cold climates could the speed of charging when the SoC is low be slower than the speed in a warmer climate. This is due to the increase of internal resistance in the battery under these conditions. Additionally, an overheated battery will have a reduced charging power, as this could preserve the lifetime of the battery [23].

Elbilforeningen estimates how the fast charging time is dependent on the temperature for typical EVs in the compact car class. Table 4.4 shows the estimated times of charging 0-80 % by using both CHAdeMO and Combo/CCS:

Temperature [°C]	**Charging time [min]**
10	30
0	45
-10	90
-20	180

Table 4.4: Charging time at different temperatures [7]

The charging times in table 4.4 is presented for batteries that are not preheated. At -20 °C will the charging time be reduced to 90 minutes if the battery is being preheated before the charging commences. From table 4.4 can it be seen that the charging time is significantly affected by the ambient temperature.

In the report *Charging into the future - Analysis of fast charger usage* by Transportøkonomisk institutt, the results of a user survey regarding long-distance travelling with EV and the use of fast chargers [23] are presented. According to the report, only a small part of EVs is being charged at fast charging stations regularly. 2% answered that they use a fast charger daily or 3-5 times each week, while 28% of the EV owners use fast chargers monthly. This represents the response from owners of all types of EVs except for Tesla. Most of the respondents (46%) replied that they fast charge their vehicles rarer than each month [23]. The survey has found that non-Tesla owners use fast charging 19 times per year on aver-

age. The few users that use fast chargers daily or several times each week is responsible for approximately 1/4 of all fast charges per year, and will most likely contribute significantly to the average number of fast charge per year [23].

In the user survey in [23], by Transportøkonomisk institutt, long-distance travelling by EV was of interest. Most of the EV owners answered that they use fast chargers for a combination of long-distance, local and regional trips. The responses on questions regarding long-distance travel show that 48% of EV owners never travel a longer distance than 300 km, while 32% never travel more than 200 km. The range of today's vehicles is one of the reasons why EV owners do not use this vehicle on long-distance trips. 55% of the respondents want a real-world range of 400 km or longer during the summer in order to use EV for vacation trips. During the winter, 50% of the respondents claimed that a real-world range of 400 km or more is acceptable for using EV on vacation trips [23]. Further, above half of the respondents answered that they would accept 1 or 2 stops with fast charging at long-distance trips as long as the wait time did not exceed 20 minutes.

4.3.2 Fast charging of road freight transport

Currently, electrified road freight transport is only in the development phase. Thus, research on how to charge these vehicles effectively is commenced. There are proposed several ways of charging electric road freight transport. One way is to use an inductive power transfer technique, which involves contact-less transfer of power between two circuits, the road charging unit and the vehicle charging unit. Another way to charge the vehicles on the move is by overhead catenary systems, similar to the technology that is currently used for trams and trains. See [35] for closer insight on these solutions. The charging method that will be assessed in this master thesis is to charge road freight transport similar to the way EVs are charged today: by charging cables.

Tesla, one of the leading manufactures of EVs, have by the launch of the truck Tesla Semi been testing charging infrastructure. Currently, a truck charging connector is under development alongside the development of the truck. Tesla claims that the truck, by the entering of the market in 2020, will be charged by four Superchargers with a maximum power output of 250 kW. This will give a peak power of 1 MW and an average power of approximately 800 kW [46]. Tesla is currently one of the manufactures that is closest to provide a full solution with both electrified road freight transport and fast charging

infrastructure to support it. It could be reasonable to assume that in the future there will many similar trucks be driving on Norwegian roads.

4.3.3 Fast charging stations

A constant development within EV technology is leading to a continued increase in the capacity of charging stations. This makes the charging of vehicles more efficient and less time-consuming. Future development is challenging to predict due to new and innovative solutions entering the market frequently. Additionally, the increase of capacity is dependent on the car manufactures adaption to the available technology for the fast chargers. Elbilforeningen states in [5] that future charging stations should offer a range of different power levels for the customer to decide the power level and the corresponding price.

The report clarifies the urgent need for charging stations due to the increase in the number of EVs. Elbilforeningen specifies that the development of new charging stations should stay ahead of the development of EVs. This might lead to superfluous charging stations for a short period. However, Elbilforeningen does believe that this is necessary in order to reach the government target of 100 % electrification of all new vehicles in 2025 [5].

In January 2019, 1,700 fast chargers were available for charging of EVs across Norway. As the total number of EVs were approximately 200,000 by January 2019, there was 118 EVs per fast charger. The report *Ladeklart Norge 2025* by Elbilforeningen states that a similar amount of EVs per charger is a reasonable target for the following years. Thus, a future scenario of 125 vehicles per charger is assumed. In order to meet the increase in EVs must approximately 8,000 new fast chargers be built within the year 2025. This results in nearly 10,000 fast chargers by 2025, which is shown in figure 4.3. Further, the number of EVs in 2050 presented in chapter 3.1.2, which was estimated to approximately 3,3 million by [51], leads to the need for 26,400 chargers by 2025 if Elbilforeningen's amount of fast chargers is required.

Figure 4.3 shows that significant development of new fast chargers must take place towards 2050. Elbilforeningen clarifies that towards 2025 the developing rate of new fast chargers must be doubled compared with previous years, to ensure an adequate amount of fast chargers per EV. In the report [5], charging of road freight transport is not specified. The reason may be the uncertainty existing around the development of electrified heavier vehicles. A scenario could be to develop parts of the areas at newly established charging

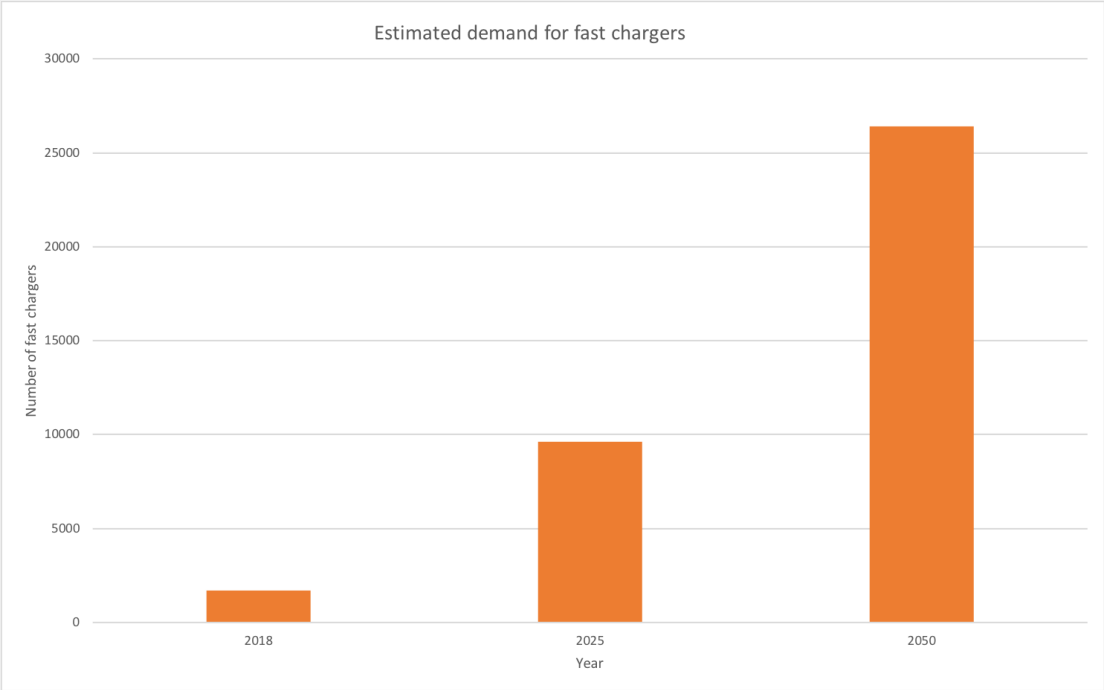

Figure 4.3: Future fast charger demand [51] and [5]

stations for charging of road freight transport.

The demand for new fast charging stations is significant in Vestfold according to [5], where only 19% of the total estimated charging need by 2025 is covered by today's charging stations. However, compared with, among others, the counties Oslo and Finnmark, which have respectively 8% and 1% of the total charging stations needed, the amount in Vestfold is not particularly low. Currently, very few charging spots are accessible for the public in Sande municipality. Figure 4.4 shows the current spots, where it can be observed that it exist a total of 13 charging spots today and further that none of these is directly linked to the main road E18. EVs in Sande, or EVs passing through Sande on route E18, can thereby benefit from the installation of fast chargers along the main road. It could be expected that vehicles passing through Sande will have the most demand for charging.

Figure 4.4 shows that most of the existing chargers are located near the centre of Sande. The municipality has currently four fast chargers, which are all located in Selvik and shown on the map in 4.4. One of Elbilforeningen's demands presented in [5] is that each municipality must have a minimum of two fast chargers. Even though Sande municipality does meet this minimum requirement, additional development of fast chargers should be

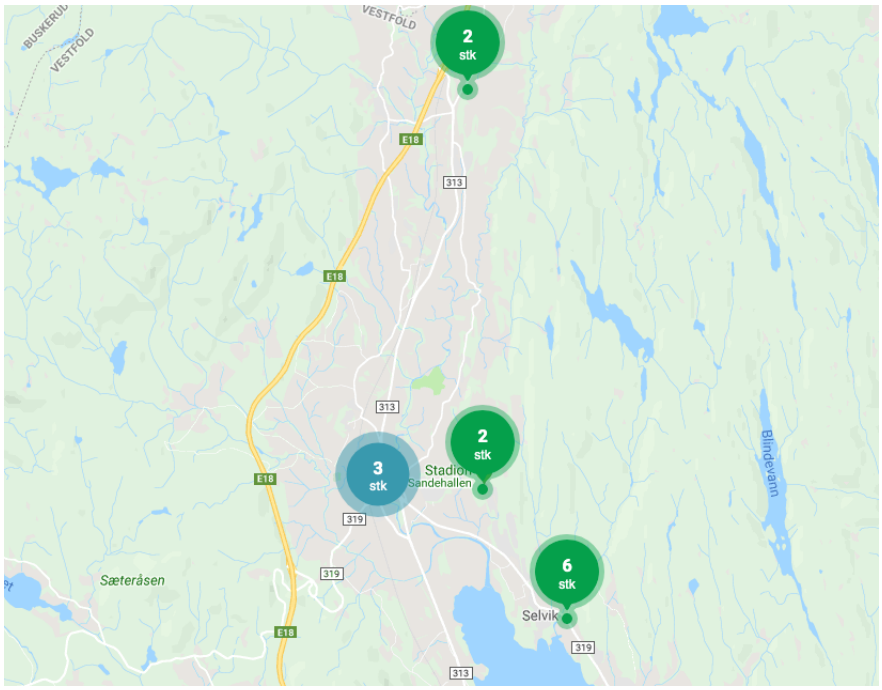

Figure 4.4: Current public charging spots in Sande [15]

considered.

Two important requirements sat by Elbilforeningen are listed below [5]:

1. Development of one fast charging park per 150 km, with a minimum of 150 kW chargers, along the national roads
2. Development of at least one fast charger per 50 km along the county roads

Trends from today's charging stations indicate that small charging stations generate longer queues than bigger charging stations, and, additionally, that the waiting time is often longer at smaller stations [5]. Therefore may bigger charging parks be beneficial. A charging park consisting of a minimum of 50 chargers, of minimum 150 kW, would equal a necessary power of around 10 MW or more. Elbilforeningen specifies that the location for the stations must be decided by evaluating which distribution grid have sufficient capacity [5] for the establishment. The development of large fast charging stations requires greater areas and should be developed in coordination with the development of infrastructure. Especially must public landowners facilitate the establishment of large fast charging stations. The

second target listed above are already reached in some parts of Norway, but there are significant parts still in the lack of charging stations.

In the EV user survey by Transportøkonomisk institutt [23], it is clear that EV users, in general, are to a certain extent pleased with current fast chargers. 59% of non-Tesla owners rated the availability or location of fast chargers to be good, whereas 86% of the Tesla owners rated similarly. The quality of fast chargers is additionally rated relatively good by the respondents, where 61% of non-Tesla owners and 94% of Tesla owners rated the quality of the stations to be good [23]. In general, Tesla owners do seem to be more satisfied with fast chargers compared to non-Tesla owners, which could have a connection with the establishment of the Tesla Supercharger network, where only Teslas are able to charge.

4.3.4 Impact of fast charging station

As fast charging stations are complex socio-technical systems, many different parameters will impact the final results [23]. Transportøkonomisk institutt presents seven parameters that will play a significant role for future fast charging stations. These are directly listed below [23]:

1. *Users needs for charging and driving and charging habits*
2. *The BEV fleets technical characteristics (battery size, fast charge capability)*
3. *Energy charged (kWh) by each vehicle*
4. *Average charge power (kW) for each vehicle*
5. *Time spent charging (min) by each vehicle*
6. *Total volume of charging (min)*
7. *Charge queues built up from the total charge volume and the time dimension*

The impact of fast charging stations on the electricity grid will depend on multiple factors. This includes the penetration of the EVs and the market share of the different types of

EVs [24]. Particularly, the impact will depend considerably on EVs' charging patterns and the capacity of the fast charging station. A significant number of vehicles charging simultaneously with high charging power can, among others, be disadvantageous for the quality of supply in a power grid [2]. In this master thesis will the impact on the reliability of supply be computed and investigated for a specific fast charging station.

4.3.5 Barriers to fast charging stations

The cost of establishing a new fast charging station is significantly high. Further, if the establishment also requires a new transformer, the total cost will be considerably higher. Development of charging stations is affected by the current tariff system in Norway. With today's solutions will the power tariff depend on, among others, the capacity installed, and thus will fast charging stations have a high power tariff [41]. Since fast charging stations that are frequently in use will have the same power tariff as fast charging stations that are used less frequently, it will be disadvantageous for the stations that are used less frequently. Fast charging stations in remote areas could thereby fail to have a profitable operation, in comparison with stations nearby cities. Elbilforeningen claims that this tariff system must be changed to ensure the operations in remote areas [5].

Another barrier for establishing fast charging stations is the investment contributions attached to new customer's connection to the power grid. The tariff system clarifies that the investment contribution must be paid by the customer that triggers the investment, as well as the other grid customers [41]. The investment contribution related to the development of new fast charging stations may be very large [5]. Especially does this apply to the creation of large stations that require high capacity, as this might require extensive upgrades of the grid. Elbilforeningen suggests in [5] that government incentives should be available for extraordinary expensive charging stations.

Chapter 5

Method

5.1 Analysis period

The analysis period of the case study is chosen to be until 2050. The reason for the selected length of analysis is the intention of studying the impact of a full electrification of the transport sector. With the governmental ambition of ending the sale of new vehicles using fossil fuel by 2025 and an assumed vehicle lifetime of 15 - 20 years, it is reasonable to assume that the transport sector not will be fully electrified until at least the year 2040 [52]. Therefore, a reasonable assumption of a fully electrified transport sector could be within the year 2050, and this is thereby the chosen analysis period.

5.2 The power grid in Sande municipality

The case study of this master thesis will be carried out in Sande municipality in Vestfold. Skagerak Nett is the DSO who has the responsibility for distributing power in this area.

NVE provides a map of, among others, overhead distribution lines in Sande, which is shown in figure 5.1 and found from [37]. The green lines represent these distribution lines with a rated voltage of $24kV$.

The distribution grid in Sande consists of several separate power grids. However, only one

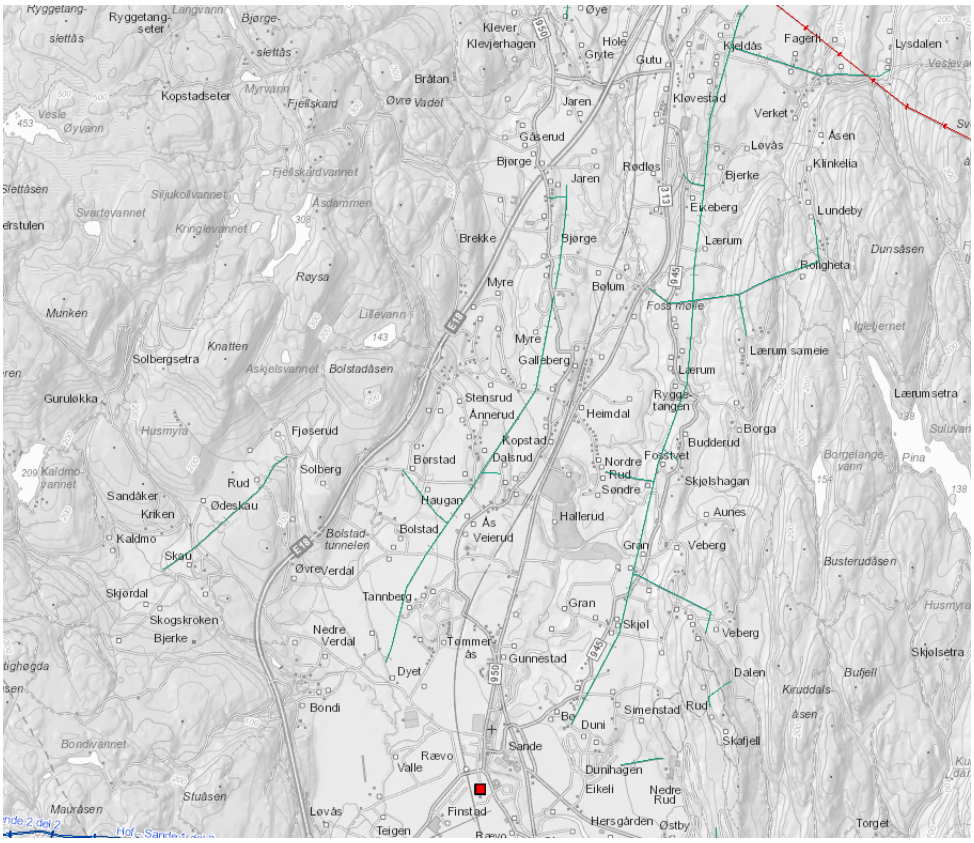

Figure 5.1: Overview of overhead distribution lines in Sande [37]

of the grids will be investigated in this case study. The exact name and location will not be presented due to the need for protecting sensitive data.

Below is a simplified one-line diagram of the power grid investigated (figure 5.2). The diagram does not show a detailed topology of the power system, thus is not the actual lengths of the power lines showed. The one-line diagram is used to be able to demonstrate the location for the transformer, specific substations, reserve connection and the general structure of the power system. The chosen alternative locations for the fast charging station are showed from this one-line diagram, marked in red (figure 5.2).

Figure 5.2 shows that the chosen alternatives for the locations of the fast charging station are spread in the power grid. Further, it can be seen where Sande transformer station and the reserve connections are located in the system. The circuit breaker, which is located directly downstream from the transformer, is not illustrated in the one-line diagram. Nor are the switches that are located between the substations.

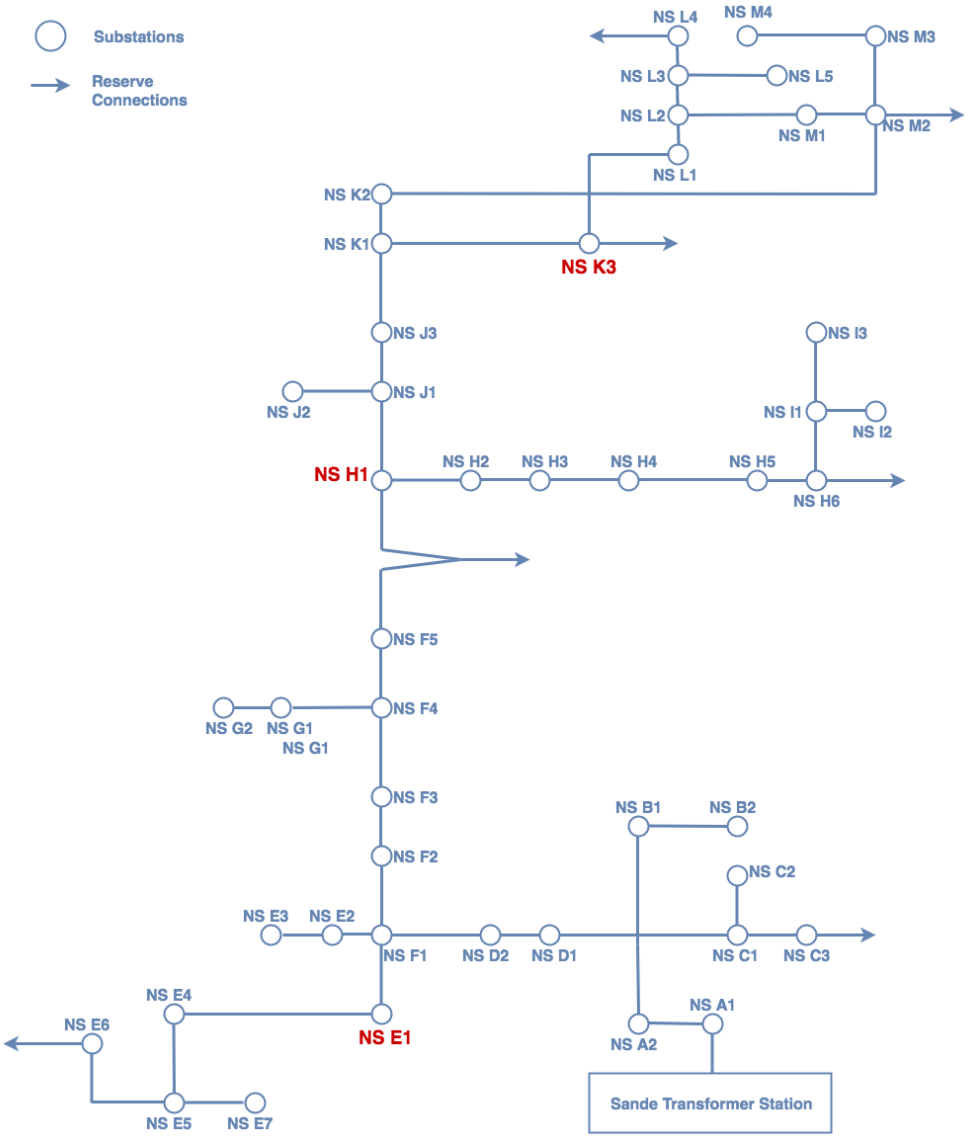

Figure 5.2: One-line diagram of the power grid in Sande

5.3 Traffic at E18 in Sande

The European route E18 runs through Sande, and a significant number of vehicles use this road each day. Statens Vegvesen provides statistics of vehicles passing specific locations on the Norwegian main roads [58]. Bolstad Tunnel at E18 in Sande is the location of interest in this master thesis.

Statens Vegvesen categorizes the vehicles passing into groups dependent on the lengths of

the vehicles, which could be of interest in this case study. However, this classification is not used due to the significantly high number of vehicles with unidentified lengths. Thus, only the total number of all vehicles passing through Bolstad tunnel will be presented.

The Average Daily Traffic (ADT) for two-way passing vehicles is showed in figure 5.3 for each month in 2018. The traffic data is found in [58].

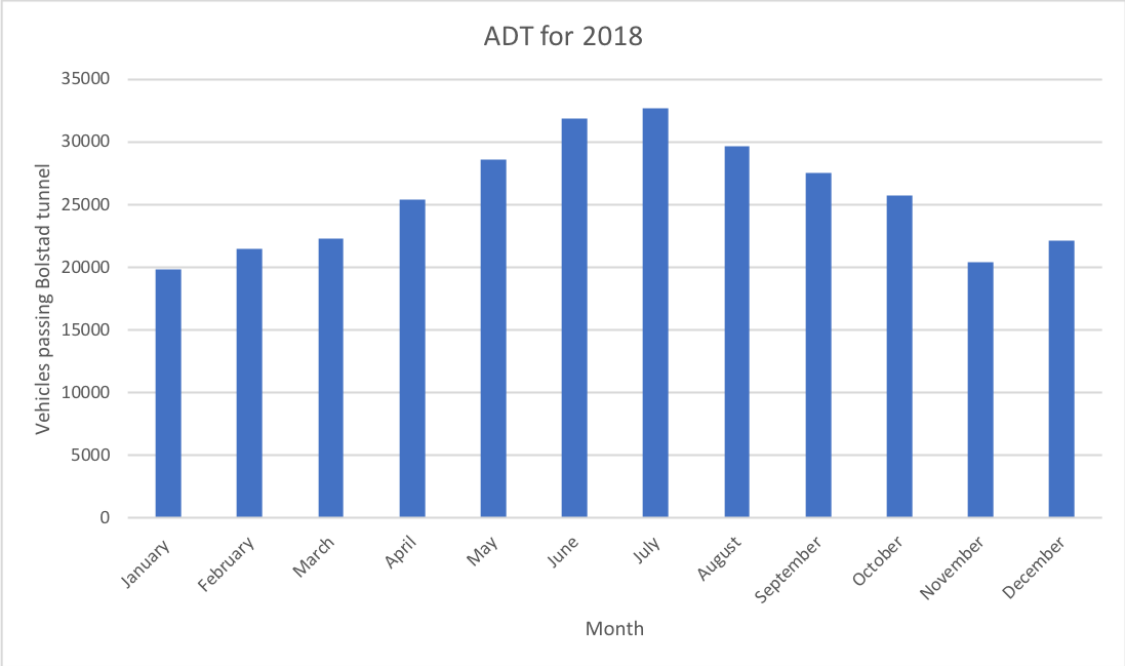

Figure 5.3: ADT for each month at Bolstad tunnel [58]

From figure 5.3 it can be seen that the ADT is at its highest values during summer, with the peak in July with an ADT of almost $33,000$. This figure shows the noteworthy difference in ADT through the year, as the minimum ADT value of approximately $20,000$ in January differs considerably from the maximum value in July.

The day with the peak ADT through the year 2018 is Friday, June 29. During this specific day, approximately $41,500$ vehicles passed through Bolstad tunnel. From the data provided by Statens Vegvesen can a trend of a weekly peak occurring on Fridays be observed [58]. The number of vehicles passing the tunnel per hour at June 29 is shown in figure 5.4

As seen in figure 5.4, the peak during this day occurs in the late afternoon, specific at 5 PM. June 29 could be seen as a 'worst-case' scenario regarding electricity demand at fast charging stations, if it is assumed that the need for charging follows the graph of vehicles

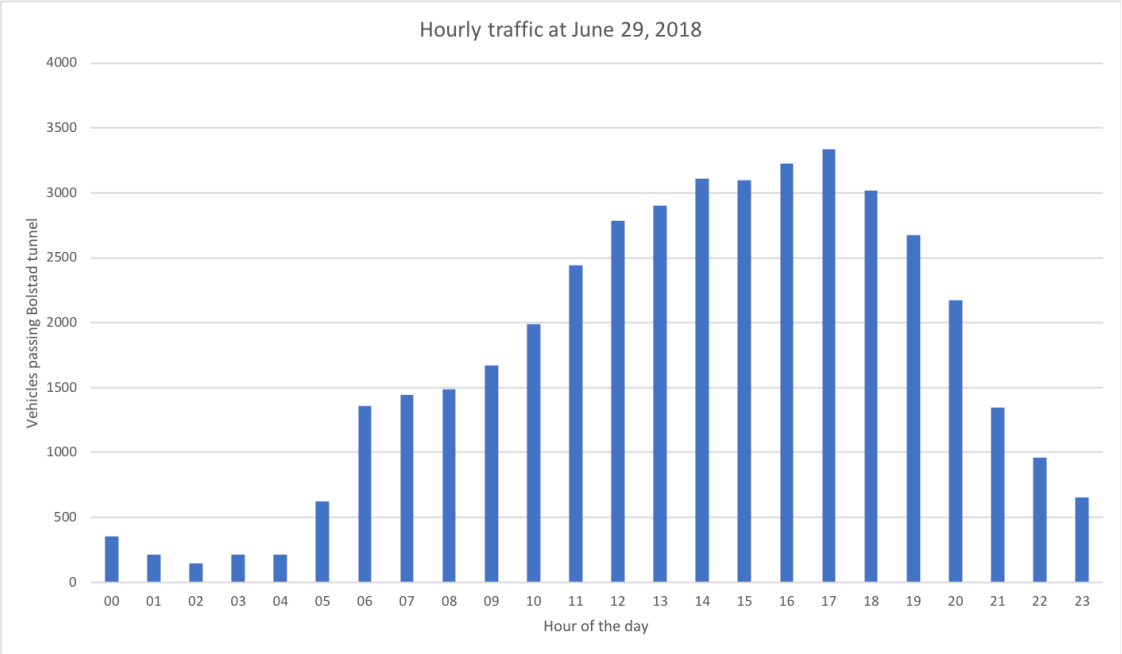

Figure 5.4: Hourly traffic at June 29, 2018 at Bolstad tunnel [58]

passing Bolstad tunnel. In this graph does e.g. hour 00 have the meaning of 00:00 to 00:59.

Future traffic at E18 in Sande will in this master thesis be assumed to follow similar trends, with an increase in the total vehicles passing. Further is it assumed that the transition from fossil fuel vehicles to EVs and electric freight road transport does not affect the trends showed in figures 5.3 and 5.4.

5.4 FASaD and the FASaD prototype

The research project *Handling of faults and interruptions in a smart medium-voltage grid* (Feil- og avbruddshåndtering i smarte distribusjonsnett), shortened the FASaD project, is a collaboration between five Norwegian distribution grid operators and SINTEF Energy Research [56]. The project investigates how smart grids can be used for reducing the total CENS of a distribution grid in a socio-economic way. The ambition is to improve the handling of faults and interruptions, among others, by calculating the theoretical potentials of different scenarios in order to improve the reliability of supply. Primarily have the project been focusing on the use of fault indicators, remotely controlled switches and self-healing

the grid. However, for this master thesis will the interest be about the theoretical change in reliability indices due to the increase in demand of a load point.

Together with the FASaD project has the FASaD prototype been developed. This is a simulation tool that is based on programming code developed by SINTEF Energy. The methodology is intended for distribution grids of 11-22 kV and is created on the basis of the RELRAD methodology. The reliability indices CENS, interrupted power and ENS are three of the main outcomes of the reliability analysis performed by using the FASaD prototype. These will be the parameters of particular interest throughout the case study.

5.4.1 Analyzes using the FASaD prototype

All analyzes of the distribution grids in Sande will be conducted using the FASaD prototype. The reliability calculations in the prototype consist mainly of three steps, given in [57] and shown in figure 5.5.

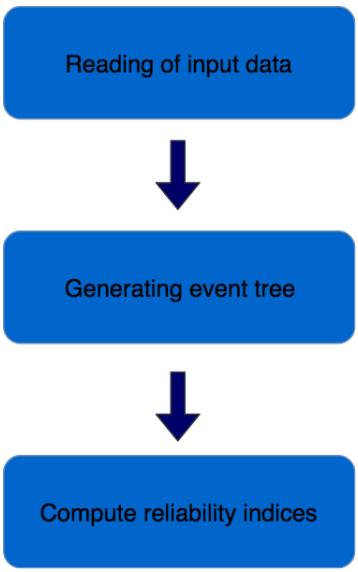

Figure 5.5: Reliability calculations in the FASaD [57]

As seen from figure 5.5, the calculations in the FASaD prototype begins by reading of the input data. The input data consist of information about all components in the system that are going to be analyzed [57]. Further, an event tree is generated for every primary fault, e.g. faults on distribution lines, based on the input data. The tree consist of all possible events, from the primary fault occurs to the fault is being isolated. This is explained more

accurate in the following section. Finally, the reliability indices are calculated from the generated event tree [57]. The simulations using the FASaD prototype will give results for all the delivery points in the grid. By summing these values, the expected annual values of different reliability indices can be found.

For generating the event three, a list of potential primary faults is made. For all the primary faults will the flow chart presented in figure 5.6 be applicable. When all primary faults occur will the circuit breaker trip before an automatic reclosure is tested [20]. If the reclosure is successful will the event be closed, as seen from figure 5.6, and the fault is seen as a temporary fault. Opposite, if the reclosure is not successful, must the fault be localized and then isolated by nearby switches. Isolating the fault location leads to the possibility of restoring the power supply to parts of the grid. Further, it can be seen from figure 5.6 that the fault gets repaired by manual reconnections, and the whole grid becomes resupplied [20].

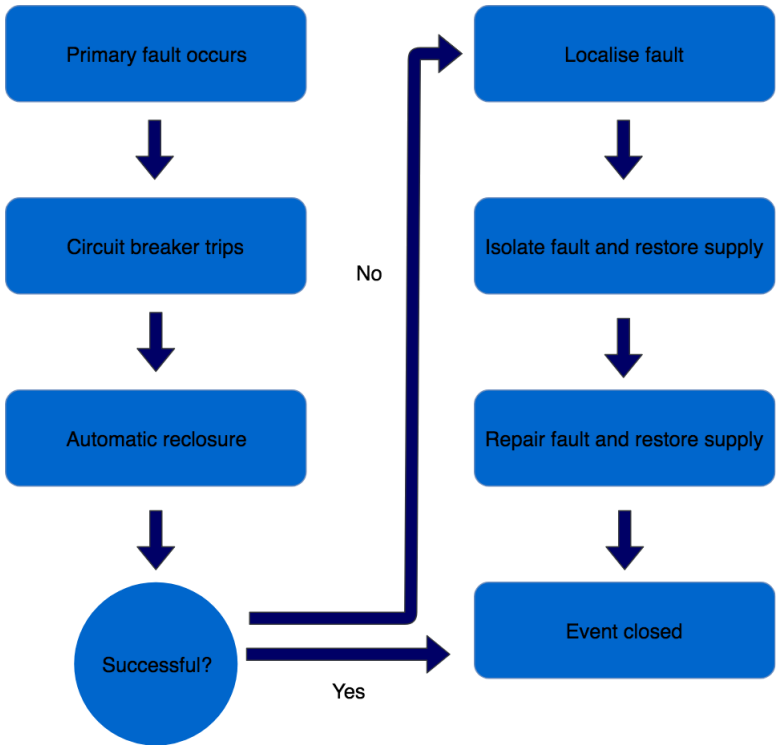

Figure 5.6: Flow chart for FASaD [20]

The FASaD prototype aims to simulate a real power grid, nevertheless must some assumptions and limitations be made. Some of these are listed below [19]:

- The circuit breaker after the transformer station has 100 % reliability
- Bidirectional power flow is not included
- Only faults on overhead lines, cables and fault indicators are included
- Isolation of fault by switches closest to the fault location
- Reserve connection to areas that are isolated from possible fault location
- Manually operation of switches where only one vehicle with workers are available
- The capacity of the reserve connection is sufficient for supplying the grid
- All loads are located at the substations

The limitations previous presented for the RELRAD model will additionally apply for the simulations in the FASaD prototype.

In the simulation using the FASaD prototype will the target of minimizing the CENS lead to a switching sequence that will ensure this. Thus, switches are selected so that the CENS will be minimal after the test reclosure [20]. Significant loads within specific customer groups will be prioritized in order to recover power supply for these delivery points. A significant extra load placed at one of the existing delivery points, as this case study will investigate, might lead to a different switching sequence.

The reliability indices that are results of the FASaD prototype simulation are calculated by using average values throughout the year. The interrupted power (kW/year), the ENS (kWh/year) and the CENS (NOK/year) are calculated by simulations in the FASaD prototype using the following formulas 3.12, 3.13 and 3.14 presented in chapter 3.3.4.

From equation 3.14 it can be seen that simulations in the FASaD prototype calculate the CENS slightly differently from the CENS calculation in equation 3.1 showed in chapter 3.3.1. Whereas equation 3.1 uses correction factors for the interruption cost of a specific hour, day and month, does equation 3.14 only use a correction factor for annual specific interruption cost. Thus, a reliability analysis using the FASaD prototype of specific days will, therefore, be lead to some calculation error.

For sectioning of the grid during a fault will the FASaD prototype, for all switches s, compute an expected value for potential CENS within the area where the fault is located after the test reclosure [19]. The expected value can be written as equation 5.1:

$$E(K_s) = \alpha_1^s c_1^s + \alpha_2^s c_2^s \tag{5.1}$$

where

c_x^s = The sum of average CENS per substation within the fault area
α_x^s = The sum of the probability of fault occurrence for all the components within the fault area

The switch with the smallest expected value $E(K_s)$ will be the switch that is chosen to trip. For every test reclosure will the affected area be reduced.

Another reliability index that is calculated by simulation using the FASaD prototype is the expected number of partial interruptions. If the circuit breaker is successfully reclosed when the fault is trying to be located, will some of the delivery points experience to only be resupplied for a small period. Then will these delivery points experience a new interruption, due to the need for further sectioning [20]. The partial interruptions per delivery point are found by FASaD simulation by the following formula (5.2) from [20]:

$$l = \sum_j \lambda_j \cdot l_j [/year] \tag{5.2}$$

where

λ_j = fault frequency for a primary fault occurring on component j
l_j = number of partial interruption by a permanent fault occurring on component j

5.5 Base load analysis

Before any load changes are being introduced to the distribution grid in Sande, the current state of the system must be analyzed. The radial grid analyzed, seen in figure 5.2, will be evaluated using the FASaD prototype and real grid data from the DSO Skagerak Nett. The base load analysis will be used as the basis of comparison for further analyzes with different locations for the fast charging station. The optimal location for the station will

be chosen as the location with the smallest percentage increase of reliability indices when the predicted load of the charging station is added.

For the base load will an assessment of reliability indices for all the delivery points in the grid be carried out. The purpose is to investigate which delivery points do initially contribute most to, among others, the total cost of interruptions in the power grid. Another purpose of evaluating all delivery points is to analyze where the different delivery points with specific reliability indices are located in the grid (figure 5.2). Further, some delivery points will be compared to illustrate and evaluate the reliability of supply. The reliability indices for the delivery points where the possible locations of the fast charging station are chosen, can for scenarios with an additional load be compared with the results from base load analysis.

5.6 Simulation scenarios

5.6.1 Optimal location for fast charging station

Three alternative locations for the development of a fast charging station are going to be analyzed using the FASaD prototype. The optimal location for this case study will be decided by minimization of reliability indices. Thus, by evaluating the increase of CENS, ENS and interrupted power for the different locations, an optimal location could be found. All locations are chosen based on its distance to route E18. The reason for the preferable short distance to the main road is, among others, Elbilforeningens requirement regarding the development of one fast charging park per 150 km along the national roads. In this case study will the possibility of the location for the charging park to be in Sande municipality be considered. To locate the fast charging station close to the centre of Sande will be disadvantageous, both considering the increased traffic towards the centre and lack of suitable areas. Additionally, when choosing the alternative location for the station will the distance to existing distribution grid be included in the decision.

The fast charging station is chosen to have a power of 10 MW. According to Elbilforeningen in [5], the fast charging stations should consist of minimum 50 charging spots for EVs and have a power demand of around 10 MW. This is the basis of the number of fast chargers chosen and the estimated power of the station. The number of fast chargers is listed below:

- **4 chargers** - Road Freight Vehicles
- **50 chargers** - EVs

There are no requirements for charging of road freight transport, which may have a connection with the unpredictable future development of heavier vehicles. In this case study is it assumed that a significant share of all road freight transport will be electrified. Thus, there is a demand for charging of heavier vehicles. At the charging parks could it be advantageous to develop charging areas that are only intended for road freight vehicles.

Changes in input parameters in the FASaD prototype

In order to simulate scenarios where a fast charging station is included in the grid must some of the input data, originally provided by Skagerak Nett, for the FASaD prototype be changed. The primary input to be changed is the average power demand per hour for the specific delivery point where the fast charging station is located for a specifically chosen scenario. The additional load due to the charging station will contribute to an enormous demand at the delivery point. In order to find the average power demand per hour, must the total power demand per year be estimated. This load profile will be found based on ADT given from Statens Vegvesen in [58]. Furthermore, the reference demand for the delivery point with the location for the fast charging station must be updated. From [43] is the reference time e.g. for the commercial customer group sat to a Monday in January at 10 AM. Thus, the updated reference demand must be found from the estimated hourly load profile of the fast charging station.

For the specific delivery point where the extra load is added will the customer composition be changed. The fast charging station is regarded as a part of the commercial customer group, also called the business customer group. As interruptions for some customer groups will contribute more to the total CENS than others, as specified in [43], is the share of the customer groups at a specific delivery point important to specify in the input parameters of the FASaD prototype.

In this master thesis is the fast charging station not considered a component that can cause a fault in the distribution grid. Hence, the significant additional load added to a chosen delivery point and the change in customer composition are the only parameters that will change the results. The annual number of interruptions in the power system will therefore

not change when the fast charging station is included in the simulations using the FASaD prototype.

Scenario 1 - Tollerud rest areas

The first location chosen to be an option for the establishment of new fast charging stations is the existing rest area at Tollerud in Sande. The rest area consist of two separate areas which are located on each side of E18, one in the northbound direction and one in the southbound direction. This is shown in figure 5.7, where northbound and southbound rest areas are named Flatbråtan and Salmakerhagen, respectively. The substation where the fast charging station will be connected to is NS H1, seen on the one-line diagram in figure 5.2. It can be observed that substation NS H1 is near 'the middle' of the grid, and further that it is located very close to a reserve connection.

Figure 5.7: Location 1 - Tollerud rest areas [37]

The FASaD prototype will be performed for the locations showed in 5.7, with an additional load due to the considered new fast charging station. Since the rest areas were built before charging stations for EVs where profitable, no room is made for this purpose. Thus, space limitations could be seen as a challenge when establishing fast charging stations at these locations. As the period of the analysis is selected to 2050, where all passenger vehicles and many road freight vehicles are predicted to be electric, it could be reasonable to place fast charging outlets at all existing parking spots. It can further be reasonable to assume that

in 30 years could an expansion of the rest area occur, as the fast charging station requires a significant area. Thus, the fast charging park required by Elbilforeningen [5] could be considered to be built on the expanded rest area. If the current areas were to be used, the space limitations will make the requirements impossible to reach. However, it currently exists separate areas for parking of road freight vehicles at both rest areas which could be used as the location for four fast chargers. Thus, the expansion of the area is assumed to occur without the need of additional areas for charging of road freight vehicles.

The fast charging station of 10 MW is intended to be split equally between the two rest areas, which gives two separate stations with a power demand of 5 MW each. However, as the two areas are very close and substation NS H1 is the closest to both stations, will a load of 10 MW be added to this substation.

Scenario 2 - Bjørge

The second scenario that will be simulated using the FASaD prototype is the establishment of a new fast charging station at an undeveloped area. The area chosen for scenario 2 is alongside E18 near Bjørge in Sande municipality, shown in figure 5.8, and the delivery point, and thereby the substation, the load will be connected to is NS K3.

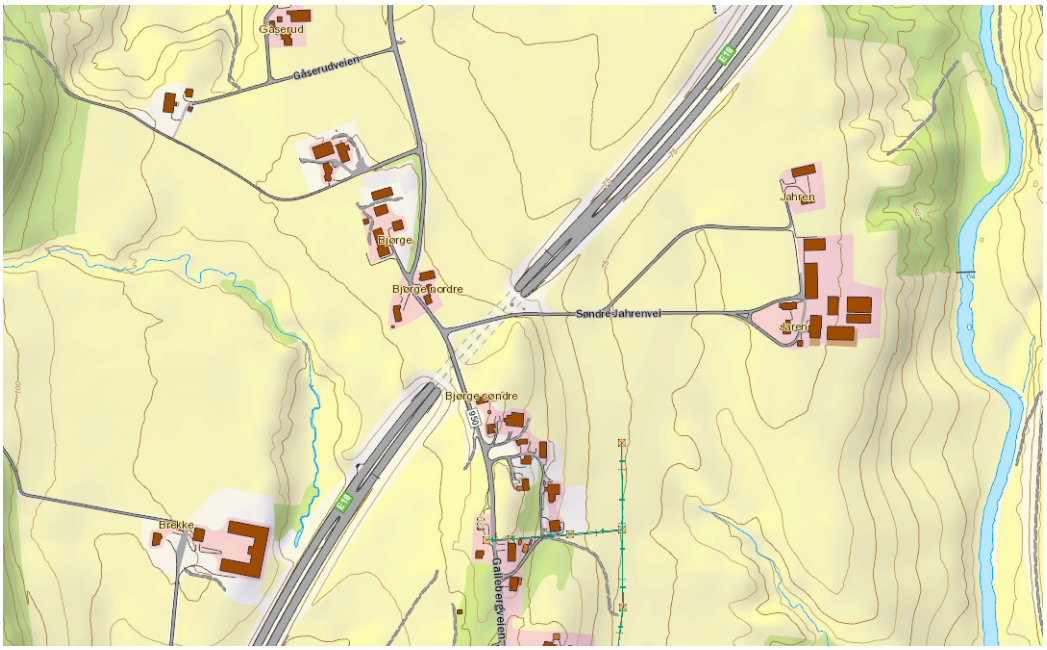

Figure 5.8: Location 2 - Bjørge [37]

It can be seen from the map in figure 5.8 that there are undeveloped areas near Bjørge which could be used for fast charging. In this case study is the realistic possibility of locating a fast charging station at this area considering, among others, landowners and other conditions not been taken into account. The area is chosen due to its location in the power grid. Since the area currently is undeveloped could the fast charging station be developed such that the use of the area is optimized. The significant size of the fast charging station that is recommended by Elbilforeningen in [5], as well as additional area for fast charging of road freight transport, should not be a problem at this location. Opposite from scenario 1, where the charging station will be at both sides of the route E18, will the charging station in scenario 2 be located at one side of the road. Thus, the exit from the main road will require more development.

The one-line diagram in figure 5.2 shows that the location for the substation is far from the transformer and the circuit breaker, and can it be observed that substation NS K3 is downstream from the substation NS H1 chosen in scenario 1.

Scenario 3 - Hanekleiva tunnel

The third location chosen as an alternative location for the fast charging station is north of Hanekleiva tunnel. From the map in figure 5.9 can this tunnel be detected, and further can it be seen that areas north of this tunnel could be available for localization of a fast charging station. The substation that will have the additional load due to the charging station is NS E1. From the one-line diagram in figure 5.2, it can be observed that NS E1 is located relatively close to the transformer and the circuit breaker in the grid. So, this substation is upstream the power grid compared to substations NS H1 and NS K3. The location is close to the road that leads directly to the centre of Sande, seen on the right side of the route E18 in figure 5.9.

Similar to the second scenario will the third scenario be located at an undeveloped area alongside one side of the route E18. Thus, similar considerations as this scenario must be taken into account if the fast charging station of similar size should be developed here.

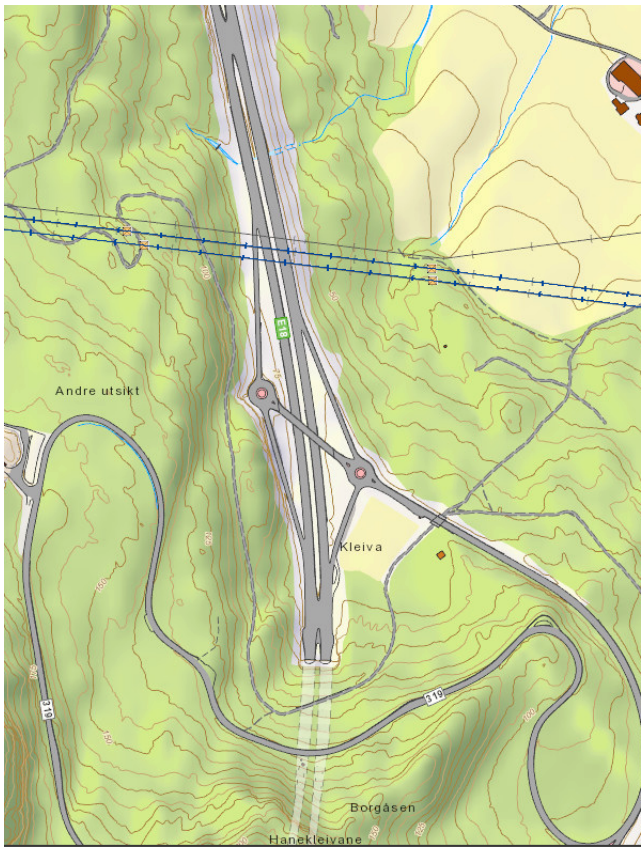

Figure 5.9: Location 3 - Hanekleiva tunnel [37]

5.6.2 Impact of a fast charging station for 'worst-case' scenario

The second part of the simulation will focus on the extent of the impact a fast charging station will have on the reliability of supply in the power grid during one specific day of the year. This day is chosen to be June 29 as this day has the peak ADT of the year 2018, described in chapter 4.3. When the peak amount of vehicles is passing Sande it is assumed a peak of the need for using a fast charger. This correlation leads to the assumption that during June 29, the fast charging station will have its maximum power demand. Thus, this day is called the 'worst-case' scenario for this case study. The analysis will be an hourly simulation in 24 steps for June 29.

The optimal location for the fast charging station that will be found with analyzes using the FASaD prototype, will be the location that will be further evaluated in this part of the case study. The purpose is to assess how the fast charging station at its optimal location will impact the power system. Even though one location is found to be the most optimal

out of the three evaluated, the impact on the power grid could still be massive for that location as well.

This analysis will be performed to evaluate how the variation of the fault frequency during a day and the load profile of a day will impact the reliability of supply. It will be investigated whether or not a high fault frequency and a significant power demand for the fast charging station will result in even higher values of reliability indices for specific hours during the 'worst-case' scenario on June 29. The reliability indices of interest are similar indices as the first part of the simulation: the CENS, the interrupted power and the ENS.

Changes in input parameters in the FASaD prototype

To evaluate the impact on the reliability of supply of the fast charging station during the 'worst-case' scenario must several input parameters for the grid in Sande be changed, before simulation by the FASaD prototype can commence. Similar to the changes in input parameters in the first part of the case study, the power demand at the chosen delivery point for the charging station must be changed. In order to assess an hourly variation during June 29 must a load profile for this day be created. Figure 5.4 shows the number of vehicles passing Sande per hour during June 29, 2018, and identical to the first part of this case study will data provided by Statens Vegvesen be used to find an estimated load profile. Furthermore, the reference demand will still be sat to the power demand at a Monday in January at 10 AM, due to [43]. The customer composition must be changed for all the hours during this day. Load data from Skagerak Nett only consist of average hourly power demand per year for each delivery point, while the estimated load data will have individual values for this specific day. Thus, this estimation will be an approximation and will include inaccurate values.

In this part of the case study must one additional input parameter be changed. This is the fault frequencies for the components in the grid. As previous specified, only faults on overhead lines, cables and fault indicators are included in the simulations using the FASaD prototype. Figure 3.2 in chapter 3.1 shows the distribution of all faults during a day. As it does not exist any statistics on the fault distribution during a day for specific components, is this data by Statnett used as input for the simulation. Previously, when finding the optimal location for the fast charging station during the whole year has the input fault frequency not be necessary to change, as average data during the year for every component

in the grid is provided by Skagerak Nett. However, when one specific day shall be simulated is the distribution of fault frequency during the day used as an input. The fault frequencies per hour during June 29. will be similar to all other days, as the distribution in 3.2 is the total distribution per hour for all days in the year. Thus, there exist some inaccuracy since the fault frequency will vary during the year.

Even though the analyzes of one single day will lead to a bit inaccurate results, the variation of hourly load data from the new fast charging station and the variation of fault frequency during a day can result in reliability data of interest of this master thesis.

Chapter 6

Results

6.1 Optimal location for fast charging station

6.1.1 Load profile of the fast charging station

Primarily, an estimation of the load profile of the new fast charging station has been performed. The load profile over a year will be used to find the new and updated demand at the delivery point where the fast charging station is located. The estimation is accomplished by using the traffic data for the Bolstad tunnel in Sande provided by Statens Vegvesen and showed in figure 5.3.

Towards 2050, an increase in both EVs and electrified road freight transport is assumed to take place. For the vehicles passing route E18 in Sande in 2050, it is assumed a similar variation for the different months as for the year 2018. From figure 5.3 is July found to be the month with the peak amount of vehicles passing Sande. Therefore, the relative amount of vehicles each month, in comparison with the peak in July, could be found. The variation of vehicles for each month during the year can be seen in table 6.1, where July is the reference month with the value 1.

As can be seen from table 6.1, there is a significant variation of vehicles passing Bolstad tunnel during the year. This must be taken into account in the estimation of the load profile per year.

Month	β_{month} **- Percentage of vehicles compared to July [%]**
Jan	0.609
Feb	0.657
Mar	0.681
Apr	0.776
May	0.875
Jun	0.974
Jul	1
Aug	0.907
Sept	0.843
Oct	0.787
Nov	0.623
Dec	0.677

Table 6.1: Montly amount of vehicles compared to July

Then, the variation of the number of vehicles during the day at randomly chosen days in July are found. As there is a significant change in driving patterns between weekdays and weekday, both a random weekday and a random day during the weekend are found. Since July is chosen as the reference month, the hourly variation of all other months are found by multiplying the hourly variation of July with the coefficients in table 6.1. This is a simplification as the hourly variation will differ some between different days during the week and for different months.

The fast charging station has been chosen to have a peak power of 10 MW. It is assumed to be unrealistic that the station only should reach this peak power in July and that for the rest of the year the peak power would be less than 10 MW. Additionally, this could indicate that a fast charging station of 10 MW was not necessary for this area since its capacity is not utilized considerably. When charging at a fast charging station, it must be expected some queue and waiting time. In order to take into account all of this, a correction of the original calculated hourly demand must be performed. Thus, the estimation of the demand is adjusted so that for all hours where initially 80% or more of the charging power was used, will now all 10 MW (100%) of the charging station be in use. At these hours will a queue occur at the station. The correction factor is, therefore, set to 1.25 and is used to correct all hours during the day. As a result of this correction will some hours have a

demand of more than 10 MW. Since this is impossible are these cases sat to 10 MW, and the extra power demand is moved to the next hour where the station is not utilized 100 %. This would be a realistic scenario, as vehicles would wait in line for some time.

The demand per hour for a weekday and a day during the weekend for the fast charging station are thereby calculated using the following formula:

$$P = \beta_{month} \cdot P_{hour,Jul} \cdot 1.25 \tag{6.1}$$

where

P = Hourly power demand [kW]
β_{month} = Correction factor for monthly variation of traffic
$P_{hour,Jul}$ = Hourly power demand in July [kW]
1.25 = Correction number for full utilization of the charging station

The results of this calculation for both weekdays and weekends of all months during a year are shown in tables A.1 and A.2 in the appendix.

There is a significant difference in power demand for a random week in July and in December, which can be seen in the comparison of the two months in figure 6.1.

From the investigation of the orange-coloured graph, which represents the power demand of one week in July, it can be seen that during multiple hours in the middle of the day is the power demand at its maximum value of 10 MW. It can be seen that this period is longer at weekends compared to weekdays. By studying the blue graph, which represents the power demand for one week in January, it can be seen that the power demand never reaches the peak value of 10 MW. The peak value for January is quite similar for both weekends and weekdays with a value of approximately 7.6 MW. However, this peak occurs at different times of the day. For both power demands shown in this figure is there a relatively stable minimum value during a few hours of the night.

When the power demand per hour for weekdays and weekends of every month in 2018 is found, can further the total energy consumption for each month be calculated. The result is given in table 6.2.

From table 6.2 it can be seen that the energy consumption reaches a peak in July, which is

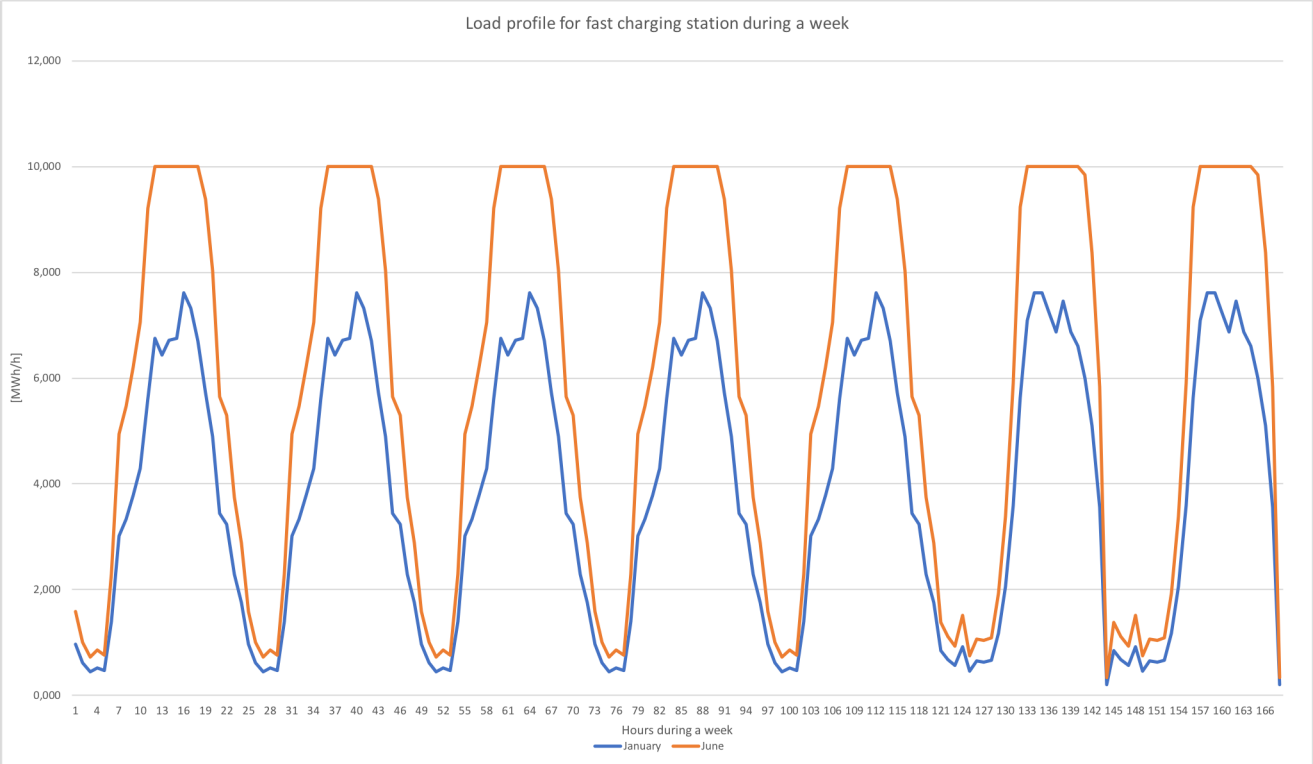

Figure 6.1: Load profile during a week

expected since the number of vehicles passing Bolstad tunnel in Sande is at its peak during this month.

When the power system with additional load due to the fast charging station is being simulated in the FASaD prototype, the input parameter of interest is the updated average power. This is found by dividing the total energy consumption per year by the number of hours during a year. The estimated total energy consumption and the average power of the fast charging station are shown in table 6.3.

This significant additional load of 4900 kW per hour, showed in table 6.3, increases the total power demand of the power system considerably. By summing the initial average power demand per hour for all the delivery points, found in table A.7 in the appendix, the total initial power demand per hour can be found to be 3607 kW.

The reference demand of the power system is 4.296 kW as this is the demand on a Monday in January at 10 AM, which is the reference time for the business customer group specified in [43]. The reference demand is found from table A.1 in the appendix.

Month	Energy Consumption Weekdays [kWh/month]	Energy Consumption Weekends [kWh/month]
Jan	2163.839	720.736
Feb	2028.058	776.836
Mar	2313.804	906.432
Apr	2514.807	1032.088
May	3073.069	1009.602
Jun	3005.986	1190.655
Jul	3192.407	1203.313
Aug	3166.450	1028.297
Sept	2588.483	1231.927
Oct	2793.055	930.316
Nov	2117.613	737.399
Dec	2195.353	1001.092
Sum	**31152.925**	**11768.693**

Table 6.2: Energy consumption of fast charging station

Total energy consumption per year [MWh/yr]	Average power demand [MW]
42921.618	4.900

Table 6.3: Energy consumption and average power of fast charging station

6.1.2 Base load analysis

A base load analysis has been performed for the grid in Sande using simulations by the FASaD prototype. The reliability indices for each delivery point in the grid are shown in table A.3, found in the appendix. To find the location of the substations in the grid, see figure 5.2. Some chosen delivery points will further be compared and investigated to evaluate the reliability of supply in the grid of Sande before any additional load due to a new fast charging station is added to the grid. The input parameters for all the delivery points are shown in table A.7, and will be used for evaluating the resulting reliability indices. In this table are the demand and reference demand for all delivery point presented, as well as the percentage distribution of the different customer groups at the substations.

When investigating the column of the number of partial interruptions per year in table

A.3, it can be seen that this number varies for the different delivery points. The number is relatively high for delivery points such as NS A2, NS C2, NS C3 and NS D1, whereas delivery points such as NS L1, NS M3 and NS M4 have a relatively low number of annual partial interruptions. This could, among others, be a result of the location of the delivery points, seen in figure 5.2. Several of the delivery points with a relatively high number are located close to the circuit breaker and the transformer, while several of those with low numbers are situated further downstream from the circuit breaker. This is a result that is expected for radial grids, where the number of interruptions during sectioning will be higher for a delivery point closer to the transformer than for a delivery point far from the transformer.

From table A.3 it can be seen that the annual interruption duration varies from approximately 74 min/year to approximately 100 min/year The substations named NS G1, NS G2 and NS J2 have the longest annual interruption duration. Some of the reason can be the location of these substations, which seen in figure 5.2 are relatively far from the transformer and reserve connections. Thus, many of the faults in the grid could cause interruptions at these delivery points. Since the optimal sectioning will ensure a minimum CENS, from equation 5.1, can the annual interruption duration for delivery points additionally be dependent on this. It can be seen in table A.3 that delivery point NS C1 have the shortest annual duration of interruptions and definitely the highest annual CENS, with respectively 74.40 min/year and 18773.81 NOK/year. This might be justified by the aim of the simulation of finding the optimal sectioning to minimize the CENS. The location of substation NS C1, which is near a reserve connection and the transformer contributes additionally to the short annual interruption duration. Additionally, it can be observed that substation NS C3, with a value of 74,45 min/year, have approximately the same annual duration of interruption as NS C1 even though the CENS is much lower. This could be due to the sectioning that leads to the restore of supply of NS C2 also will lead to the restore of supply for NS C3 in many cases.

From a further investigation of substation NS C1, it can be observed that this substation have the largest demand and reference demand, with respectively 463.745 kW and 897.010 kW, and, as previously mentioned, have additionally the highest annual CENS. This could, among others, be explained by equation 3.14 where reference demand P_{ref} contributes to the expected annual CENS. From this equation, it can also be seen that a correction factor for annual specific interruption cost will affect the calculated CENS for a delivery point. Thus, the share of the different customer groups represented at a delivery point will

additionally impact the CENS.

If two delivery points have the same power demand and fault frequency will the resulting interrupted power be equal as well. This can be seen from equation 3.12. Verification of this can e.g. be seen by comparing reliability indices for NS L1 and NS K2 in table A.3, where the ratio between the interrupted power and the power demand at the two delivery point will be equal to each other, and equal to the common annual number of interruptions. This is shown in the following calculation.

$$\frac{P_{interr,L1}}{P_{L1}} = \frac{P_{interr,K2}}{P_{K2}}$$

$$\frac{10.10}{16.80} = \frac{10.54}{17.53} = 0.60$$

It can be seen from this calculation that for equal power demand and the annual number of faults, will the interrupted power be equal.

Finally, when investigating the ENS of all delivery points in the grid it can be observed that substation NS C1, which have the highest power demand and CENS, also have the highest ENS with approximately 575 kWh/year. However, as equation 3.14 shows, there are several factors that affect the CENS. From table A.3 it can be noticed that substations NS C3 and NS L5 have approximately the same annual ENS, with respectively 78.68 kWh/year and 78.28 kWh/year. Even though the ENS is almost equal, does the CENS differs for these two substations. NS C3 has an annual CENS of 5170.93 NOK/year, while NS L5 has a cost of 1641.79 NOK/year. The share of customers at the two substations could be one of the reasons for the different values of CENS. While all customers at substation NS L5 are within the residential customer group, are the customer at substation NS C3 divided between the residential, the commercial and the public sector customer group, seen in table A.7. As the CENS is different for the different customer groups could the CENS vary significantly for the substations. As earlier mentioned, the location of the substation can additionally impact the CENS for the delivery points.

Further, in this case study will the total sum of reliability indices at all delivery points in the power system be of interest. Table 6.4 shows the total sum of the annual CENS, the annual interrupted power and the annual ENS.

	Power Grid
Annual interruption cost [NOK/yr]	156 054
Annual interrupted power [kW/yr]	1670.280
Annual energy not supplied [kWh/yr]	3732.206

Table 6.4: Reliability indices for base load scenario

The reliability indices in table 6.4 will change when an additional load due to the fast charging station is added to the power system. Parameters such as annual partial interruptions could also change due to change in the switching sequence of the grid during a fault. However, as this is included in the calculation of some of the parameters in table 6.4 are these three parameters considered sufficient for further comparison between base load scenario and scenarios with different locations for a new fast charging station.

6.1.3 Scenario 1

In scenario 1 is the fast charging station of 10 MW located at Tollerud rest area, and the additional load is therefore added in the FASaD prototype simulation at delivery point NS H1. The results, presented in table 6.5, show an increase in the annual CENS, annual interrupted power and annual ENS compared to the base load scenario.

	Scenario 1	**Increase compared to base load scenario**
Annual interruption cost [NOK/yr]	525 642	369 588
Annual interrupted power [kW/yr]	4615.985	2945.700
Annual energy not supplied [kWh/yr]	9894.818	6162.612

Table 6.5: Total sum of reliability indices for scenario 1

From table 6.5 can it be seen that all three of the reliability indices presented are increasing significantly compared to the base load scenario. Further, table 6.6 and 6.7 show the comparison of some of the reliability indices of the affected delivery point before and after the fast charging station is added. It can, among others, be seen that the average and annual interruption duration is decreased for scenario 1 compared to the base load scenario.

The comparison of the annual CENS, found in table 6.7, shows a massive increase for

Delivery point	Annual number of partial interruptions [/yr]	Average interruption duration [min/interruption	Annual interruption duration [min/yr]
NS H1 Without extra load	1.201	91.335	84.811
NS H1 With extra load	1.272	84.020	78.018

Table 6.6: Reliability indices at NS H1 with and without fast charging station - Part 1

delivery point NS H1 when the fast charging station is included in the simulation. Further, it can be seen that the annual number of interruptions is constant. Similar to the annual CENS are the annual interrupted power and the annual ENS increasing massively for scenario 1.

Delivery point	Annual interruption cost[NOK/yr]	Annual number of interruptions [/yr]	Annual interrupted power [kW/yr]	Annual energy not supplied [kWh/yr]
NS H1 - Without extra load	5595.247	0.601	19.467	45.772
NS H1 - With extra load	383272.936	0.601	2965.172	6413.572

Table 6.7: Reliability indices at NS H1 with and without fast charging station - Part 2

6.1.4 Scenario 2

In scenario 2 is the fast charging station located at substation NS K3, some distance away from the transformer and the circuit breaker. Simulations using the FASaD prototype gives the sum of reliability indices for the power grid shown in table 6.8. This table shows a significant increase in annual CENS, interrupted power and ENS compared to the base load scenario.

Tables 6.9 and 6.10 present the change in all the reliability indices for substation NS K3.

	Scenario 2	**Increase compared to base load scenario**
Annual interruption cost [NOK/yr]	559 354	403 300
Annual interrupted power [kW/yr]	4615.99	2945.71
Annual energy not supplied [kWh/yr]	10913.68	7681.47

Table 6.8: Reliability indices for scenario 2

Delivery point	**Annual number of partial interruptions [/yr]**	**Average interruption duration [min/interruption**	**Annual interruption duration [min/yr]**
NS K3 Without extra load	0.929	93.809	87.108
NS K3 With extra load	0.939	93.765	87.067

Table 6.9: Reliability indices at NS K3 with and without fast charging station - Part 1

Delivery point	**Annual interruption cost[NOK/yr]**	**Annual number of interruptions [/yr]**	**Annual interrupted power [kW/yr]**	**Annual energy not supplied [kWh/yr]**
NS K3 - Without extra load	920.743	0.601	16.723	40.385
NS K3 - With extra load	404013.873	0.601	2962.428	7150.851

Table 6.10: Reliability indices at NS K3 with and without fast charging station - Part 2

It can be observed, from table 6.9, that the annual number of partial interruptions increases marginally for scenario 2. Furthermore, the comparison of annual and average interruption duration for base load scenario and scenario 2 shows a marginal decrease when the fast charging station is included.

Significant increase in the annual CENS, the annual interrupted power and the annual ENS for scenario 2 compared to the base load scenario are shown in the table 6.10. Similar to

scenario 1 is the annual number of interruptions unchanged after the fast charging station is included in the simulation.

6.1.5 Scenario 3

In scenario 3 is the fast charging station of 10 MW located at substation NS E1, which is the chosen location that is closest to the circuit breaker and the transformer in this power system. The results of the simulations in the FASaD prototype regarding the total sum of chosen reliability indices are presented in table 6.11. Similar to results for scenario 1 and 2 are the annual CENS, the annual interrupted power and the annual ENS increasing significantly compared to the base load scenario. All three scenarios will be compared in the next section.

	Scenario 3	**Increase compared to base load scenario**
Annual interruption cost [NOK/yr]	541 835	385 781
Annual interrupted power [kW/yr]	4615.99	2945,71
Annual energy not supplied [kWh/yr]	10351,29	7119,08

Table 6.11: Reliability indices for scenario 3

The substation NS E1 will experience a considerable change in many of the reliability indices due to the new fast charging station. Tables 6.12 and 6.13 shows these changes. First, it can be observed that the annual number of partial interruptions decreases. Further, a significant increase in the annual and average interruption duration can be detected from table 6.12. The change in the switching sequences is the reason that annual interruption duration will increase for this scenario, as the CENS for the power grid will be minimized at this specific switching sequence. Inspection of table 6.13 shows trends similar to tables 6.7 and 6.10. There is, among others, a massive increase in the annual CENS when the fast charging station is added to substation NS E1. Additionally, a significant increase in both the annual interrupted power and annual ENS can be observed from table 6.13.

Delivery point	Annual number of partial interruptions [/yr]	Average interruption duration [min/interruption	Annual interruption duration [min/yr]
NS E1 Without extra load	1.710	82.453	76.563
NS E1 With extra load	1.589	86.225	80.065

Table 6.12: Reliability indices at NS E1 with and without fast charging station - Part 1

Delivery point	Annual interruption cost[NOK/yr]	Annual number of interruptions [/yr]	Annual interrupted power [kW/yr]	Annual energy not supplied [kWh/yr]
NS E1 - Without extra load	139.068	0.601	55.587	117.991
NS E1 - With extra load	385952.288	0.601	3001.292	6662.062

Table 6.13: Reliability indices at NS E1 with and without fast charging station - Part 2

6.1.6 Determination of optimal location for fast charging station

To determine which of the three chosen locations that will be the optimal location for the fast charging station, with respect to the reliability of supply, a comparison of the results for the three scenarios is conducted. The percentage increase of annual CENS, annual interrupted power and annual ENS are presented in figure 6.2.

From figure 6.2, it can be observed that the increase in the annual interrupted power is equal for all three scenarios, with a percentage increase of 176 %. Since the additional power demand due to the new fast charging station and the fault frequency is similar for all the scenarios, shows the equation for calculating the interrupted power in the FASaD prototype (equation 3.12) that different location will get equal interrupted power. Thus, the indices that will decide which substation will be the best location for the fast charging station are the annual CENS and the annual ENS. From figure 6.2 can it be noticed that the

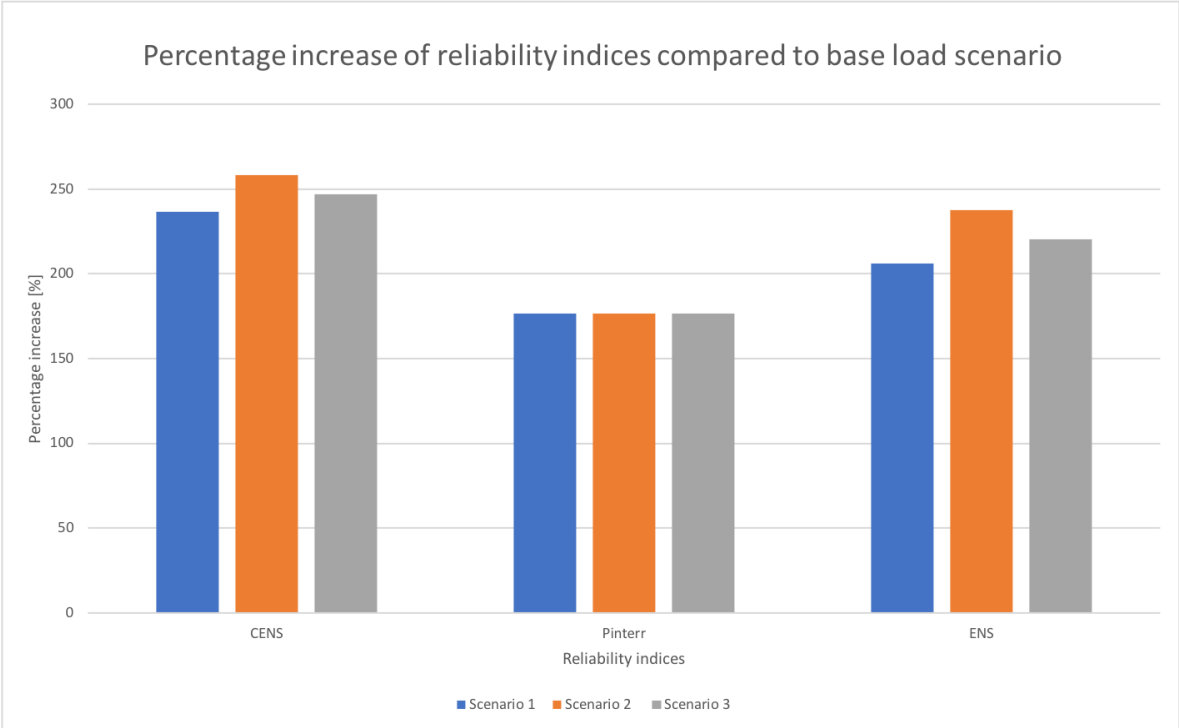

Figure 6.2: Percentage increase of reliability indices compared to base load scenario

scenario with the highest CENS and ENS is scenario 2, with respectively 258% and 237% increase, while it can be seen that the reliability indices for scenario 3 have considerably lower values, with respectively 247% and 220% increase for CENS and ENS. Scenario 1, to locate the fast charging station at Tollerud rest area, is the optimal location based on the smallest increase of reliability indices in the power grid. However, this scenario also has a massive increase in reliability indices, with respectively 236 % and 206% increase for CENS and ENS.

The optimal location of the fast charging station is dependent on which location will lead to the most optimal switching sequence. Thus, the switching sequence that minimizes the total CENS. The additional power demand due to the fast charging station can cause a change in the switching sequence, which will cause a change in the interruption duration at delivery points and thereby the CENS. The fast charging station at Tollerud rest area is located close to a reserve connection. The FASaD prototype logs, among others, all the openings and closings of all switches in the power grid. From this can it be found that when the extra power demand of 4.9 MW per hour is added to Tollerud rest area at substation NS H1, the switch between NS H1 and NS F5 is the first to open when the fault localization

starts. Secondly, the switch between NS H1 and NS J1 opens. As the power demand of the fast charging station is prioritized due to the purpose of minimizing the total CENS in the power grid, will the power be restored at this delivery point, while the localization of the fault continues. For scenario 2, where the fast charging station is located at substation K3, the switching sequence is different. A switch between NS K1 and NS K3 will be the first to open after the circuit breaker has failed the test with automatic reclosure. Then, a switch between NS F1 and NS F2 opens. By comparison of the switching sequence for the first switches for scenario 1 and 2, it can be found that the sequence changes due to the change of location for the fast charging station. For scenario 3, which is located closest to the transformer, are the first switches that will be open after a fault in the power system found to be between substations NS E1 and NS F1, and thereafter between NS F5 and NS H1. This difference in switching sequences leads to variation in annual interruption duration for the three scenarios, which will cause variation in the total annual CENS and ENS. As scenario 1 has the lowest total annual CENS of the power system, will this switching sequence, due to the fast charging station's location at substation NS H1, be the most optimal. Substation 1 will be resupplied with power shortly after a fault has occurred.

As the FASaD prototype simulation aims for minimizing the total CENS in the power grid will the increased CENS due to the fast charging station be as low as possible for all simulated scenarios of the power grid. A closer look at the increase of CENS at the three scenarios have been shown in table 6.14. Here can the increase in CENS at the specific substation where the fast charging station has been located for each scenario be compared with the total increase in CENS for that scenario.

Scenario	**Increase in CENS at substation with fast charging station [NOK/yr]**	**Total increase in CENS in the power grid [NOK/yr]**
Scenario 1	377 677	369 588
Scenario 2	403 093	403 300
Scenario 3	385 813	385 781

Table 6.14: Increase in CENS

From table 6.14 it is clear that most of the increase in CENS for the whole power grid is from the increase at the specific substation where the load from the fast charging station is added. In fact, it can be seen that the increase in CENS at the substations with fast charging stations is higher than the total increase in the power grid for both scenario 1

and scenario 3. This is due to a decrease in the CENS for other substations, due to the change in switching sequence. Tables A.4, A.5 and A.6 in the appendix show the CENS for each delivery point for the three scenarios. For example, it can be observed from a comparison between table A.3 and table A.4 that the substations close to substation NS H1, where the fast charging station is located, have a significantly reduced CENS. This involves substations such as NS H2, NS H3, NS H4, NS J1 and NS J3. When comparing the two tables, it can be seen that all substations will have some reduction in the resulting CENS. On the other hand, comparing the CENS at each delivery point for scenario 2 and the base load, it can be observed that most of the delivery points have an increased value of CENS when the fast charging station is included in the simulation. Only two substations, NS M1 and NS M3, which are close to the substation with the additional charging station load have an increased CENS.

By observing table 6.14 it can be seen that scenario 1, which have the smallest increase in CENS at the substation where the fast charging station is located, also have the smallest increase in the total CENS in the system. The largest increase for the substation occurs for scenario 2, which also have the largest increase of CENS for the whole power system. Thus, the increase of CENS at the substation with the additional load from the charging station seems to be very significant for the increase in CENS for the whole power system.

To summarize, the location of the fast charging station at substation NS H1, hence, Tollerud rest areas, is the most optimal location for the fast charging station when considering the impact of reliability of supply in the power system. Scenario 2, longest away from the circuit breaker, have a decreased reliability of supply compared to scenario 3, which is located closest to the circuit breaker. However, scenario 1, which is located very close to a reserve connection and in between the two other scenarios, have the best reliability of supply.

6.2 Impact of a fast charging station for 'worst-case' scenario

6.2.1 Load profile and fault frequency for 'worst-case' scenario

To calculate the reliability of supply for the day with the assumed maximum power demand at the substation must the load profile for this day be estimated. This is accomplished by using the same procedure as explained in chapter 6.1.1, when the load profile during the whole year was found for the fast charging station. See this chapter for a more detailed explanation of the approach.

As June 29 is the day with the peak ADT during 2018, and thereby the day with the assumed maximum power demand, will the traffic data for this day be used for the creation of a load profile. The number of vehicles per hour driving through Bolstad tunnel in Sande is shown in figure 5.4. The peak number of vehicles passing is between 5 PM and 6 PM, and this hour is, therefore, sat to the reference value 10 MW, as this is the peak load of the fast charging station. The load at all other hours at June 29 will be found by studying the relative amount of vehicles passing at the specific hour compared to the number of vehicles between 5 PM and 6 PM. As this would lead to an unrealistic scenario where the fast charging station only will have a peak load of 10 MW during one hour that day, is all hours multiplied with the correction factor 1.25. This and further changes are performed precisely as explained in chapter 6.1.1. The average power demand for specific hours, thus the energy consumption per hour, for the fast charging station is presented in table A.8 in the appendix. The following figure 6.3 shows the estimated load profile on June 29. In this figure does e.g. hour 1 mean 00:01 to 01:00.

In addition to showing the load profile at the fast charging station during the 'worst-case' scenario in figure 6.3, the fault distribution during a day is shown. Since both these parameters are used for the calculation of the annual interrupted power, the ENS and the CENS, could the variation of these during a day cause a variation in the reliability indices. From figure 6.3 it can be noticed that the two graphs for load profile and fault distribution during June 29 have similar trends. Both profiles have their minimum values during the night, between 2 AM and 5 AM. Furthermore, both graphs increase significantly during the morning. It can be observed that the peak number of faults occurs at 10 AM, and further that the number of faults decreases during the afternoon. The graph representing the load

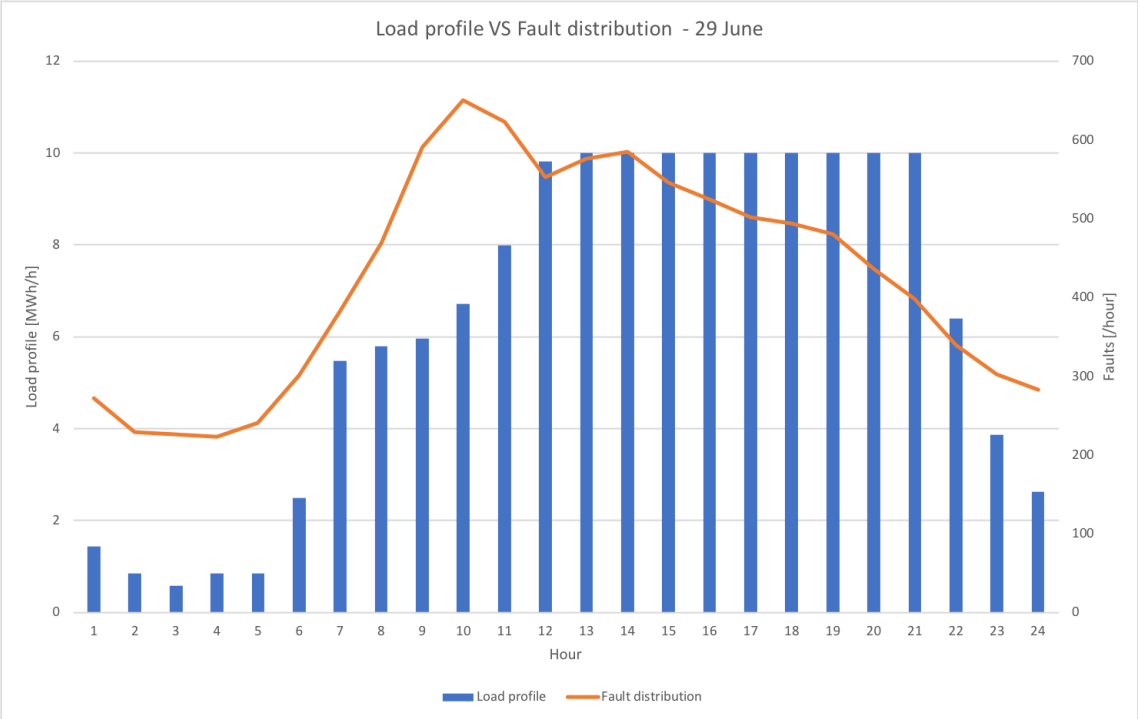

Figure 6.3: Power demand of fast charging station at June 29.

profile of the fast charging station differs from the graph of fault distribution during these hours. When the load at the fast charging station is stable at 10 MW, from 1 PM to 9 PM, the number of faults decreases. At the peak number of faults at 10 AM it can be seen that the load at the fast charging station not yet have reached its maximum value.

This change of fault frequency and load profile during June 29 will be used as input in the FASaD prototype for finding the impact the fast charging station will have on the reliability of supply in the power system in Sande. The different impact of the two variables will be evaluated in the next section.

6.2.2 Impact on reliability indices at June 29

The simulations by the FASaD prototype gives, among others, summarized values of reliability indices of all delivery points in the power grid. The reliability indices of interest for this part of the case study are the interrupted power per hour, the CENS per hour and the ENS per hour. Since the FASaD prototype initially gives results per year for all

the reliability indices, the result must be corrected so that hourly values are found. Thus, the annual result for CENS, ENS and interrupted power found by calculations using the FASaD prototype will be divided by 8760, the number of hours in a year.

The resulting graph for the CENS in the 'worst-case' scenario on June 29 is shown in figure 6.4.

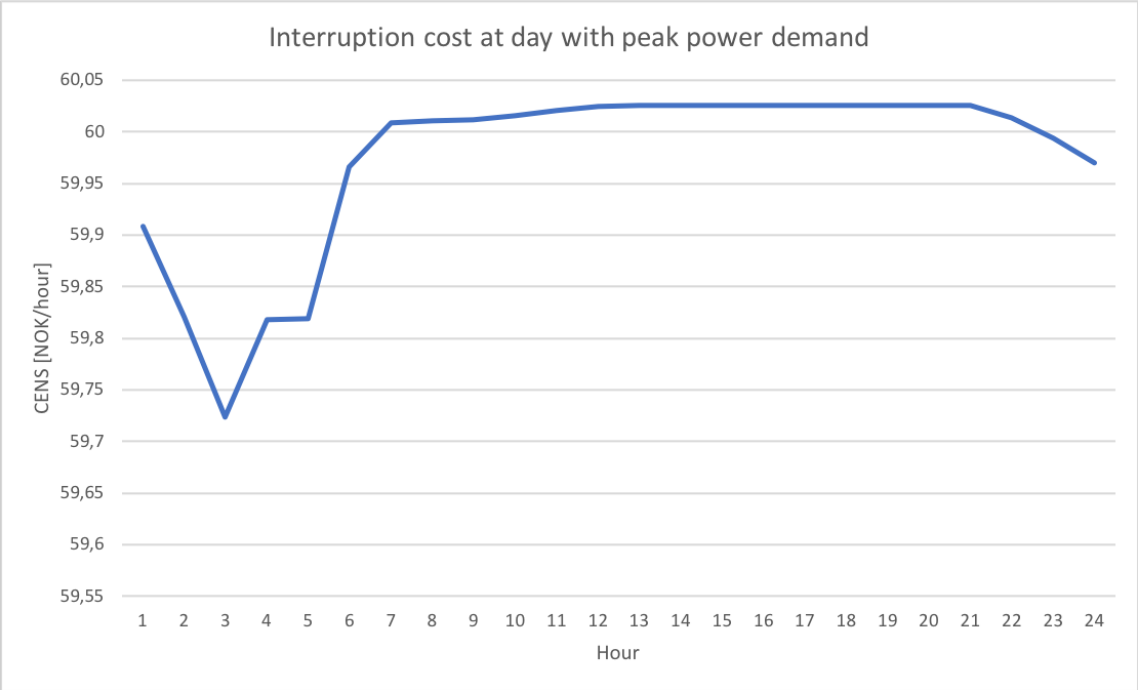

Figure 6.4: Interruption cost at day with peak power demand

From figure 6.4 it can be seen that the CENS is almost constant during the day. The cost varies from 59.72 NOK/hour to 60.03 NOK/hour. The reason for this can be explained by equation 3.14 for calculation of CENS in the FASaD prototype. The reference demand is one of the input parameters, and as this is constant for the whole simulation will the reference demand not contribute to an hourly change in the CENS. However, as the variation in the actual demand at the fast charging station will lead to small changes in the customer distribution at the substation, will this affect the CENS per hour. Since the FASAD prototype uses a correction factor for annual specific CENS will the resulting CENS per hour be inaccurate. It could be possible to find more correct results for the CENS per hour as all the correction factors are known. The correction must be performed for all customer groups at all delivery points for all hours. Thus, this will be a very time-consuming process and will not be performed in this master thesis. However, an example of the calculation

that must be performed will be shown in the following section.

The FASaD prototype uses average correction factors for specific hours, days and months. All correction factors for all six customer groups can be found in [43]. This includes the average correction factors for a year. From table A.9 in the appendix can it be seen that the hours 1 PM until 9 PM have equal CENS per hour. Correction of the CENS for delivery point NS H1 where the fast charging station is located can be performed using the following formula 6.2:

$$CENS_1 = CENS_0 \cdot \frac{f_{Ch,1} * f_{Cd,1} * f_{Cm,1}}{f_{Ch,0} * f_{Cd,0} * f_{Cm,0}} \tag{6.2}$$

where

f_{Ch} = Correction factor for interruption cost (NOK) in hour h
f_{Cd} = Correction factor for interruption cost (NOK) in day d
f_{Cm} = Correction factor for interruption cost (NOK) in month m

Further, 0 is representing the average correction factors which the FASaD prototype uses and 1 is representing the specific correction factors for the specific day.

Results from the calculations of the contribution to the total CENS, by the different customer groups at substation NS H1, for two different hours at June 29 are shown in table 6.15. In this calculation have the percentage distribution of the two customer groups at the substation been included to find the correct total CENS for this substation.

Hour	**Business CENS [NOK/hour]**	**Public CENS [NOK/hour]**	**Total CENS for substation**
1 PM	92.250	0.0421	92.292
9 PM	27.675	0.0182	27.693

Table 6.15: CENS per hour for a substation

The FASaD prototype found that the total CENS for this substation was 43.773 NOK/hour for, among others, the hours 1 PM and 9 PM. Thereby, it can be seen that to estimate a more realistic CENS for a delivery point is relevant to include in a comprehensive study of the distribution of CENS during a day, as the change is significant. At substation NS H1 is the fast charging station responsible for 99.9 % of the total power demand. Thus,

almost all of the CENS comes from the commercial customer group. This will naturally be different at other substations. As this calculation must be performed for all delivery points in the grid, the total CENS for each hour can vary considerably from the CENS found directly from the simulations using the FASaD prototype.

The graphs for the ENS and the interrupted power during June 29 are shown in the following two figures, 6.5 and 6.6.

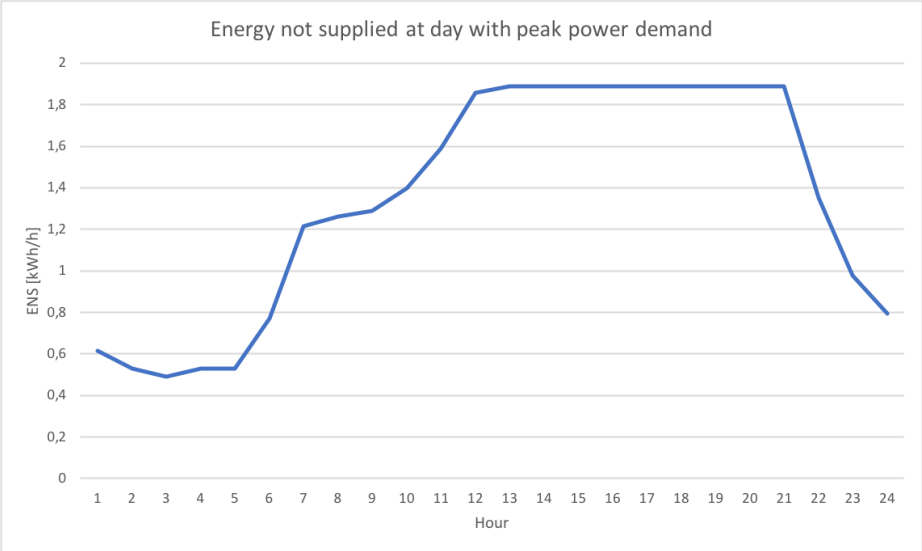

Figure 6.5: ENS at day with peak power demand

Unlike the small variation in CENS found from the FASaD simulation, do the reliability indices in 6.5 and 6.6 vary significantly during the day. It can be observed that figure 6.5 and 6.6 have similar shapes, which also can be seen in the graph for CENS in figure 6.4.

An important observation is that all of the graphs representing the reliability indices during June 29 have a similar shape as the load profile for the fast charging station during this day. The resulting interrupted power and the ENS are dependent on the power demand and the fault frequency in the grid. As the charging station is responsible for a significant part of the total power demand in the grid, the load profile for charging station impacts these reliability indices considerably. Figure 6.7 shows that the graph representing the interrupted power during a day for the entire power grid has a similar shape as the estimated load profile for the fast charging station.

Thus, it seems like the load profile impact the reliability indices, whereas the change in fault frequency during the day has a small impact. A verification of this can be seen from

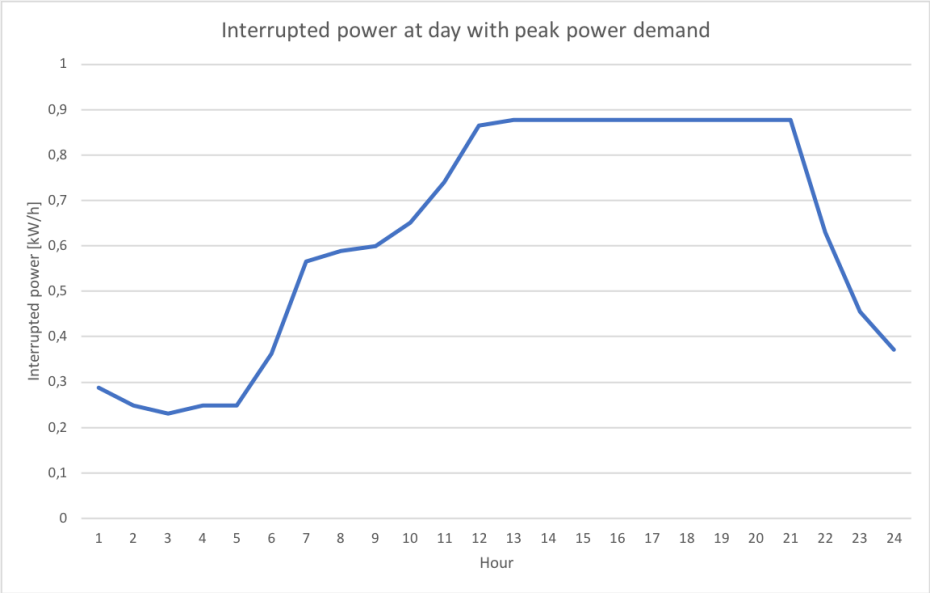

Figure 6.6: Interrupted power at day with peak power demand

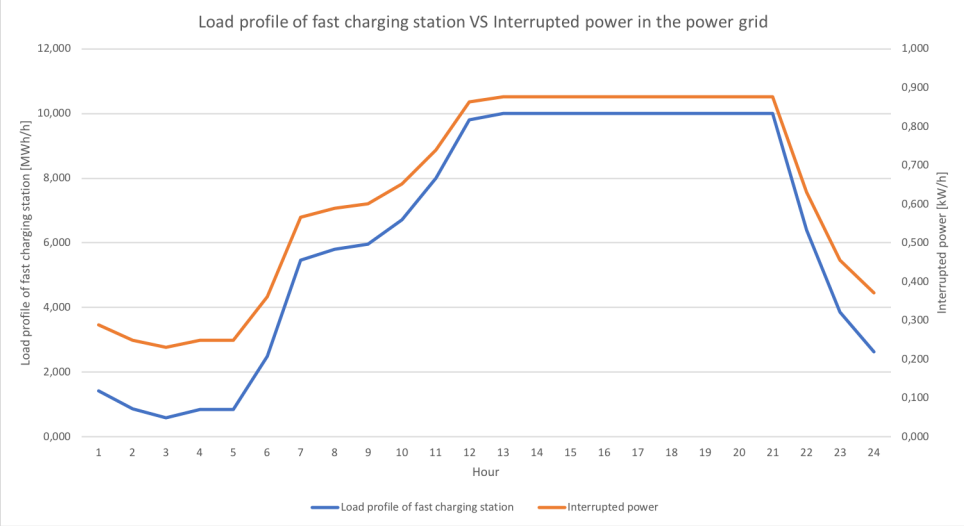

Figure 6.7: Load profile for fast charging station and interrupted power of the grid

the comparison of table A.8 and A.9 in the appendix, where all three reliability indices have constant values when the demand is 10 MW at the fast charging station. From figure 6.3, it can be seen that the number of faults decreases while the load profile is constant. This means that the change in the fault frequency during the day will have minimal impact on the reliability of supply of this power system. Even if the values of the reliability indices have included more decimals than showed in table A.9, no difference between the hours 1

PM to 9 PM can be detected.

Chapter 7

Discussion

In this chapter will the results of the reliability analyzes performed by the FASaD prototype be discussed. First, the results that are used as a basis for deciding the optimal location for the fast charging station will be reviewed, and then will the results for the analysis of the 'worst-case' scenario be discussed closer. Finally, the assumptions and limitations that are made before performing the reliability analyzes will be thoroughly discussed.

7.1 Optimal location for fast charging station

To find the power demand of the fast charging station is essential before a reliability analysis can commence. The load profile used in this master thesis is estimated based on traffic data provided by Statens Vegvesen. This is due to very limited demand data from existing fast charging stations and further that few research reports have currently been published on future fast charging demand. In this case study is the capacity of the fast charging station decided based on Elbilforeningen's recommendations. The amount of EVs and road freight vehicles that can be charged simultaneously are thereby found from the determined peak power at the charging station. Thus, an exact estimation of the future traffic at route E18 through Sande is not necessary to find. It is assumed that the traffic data will show similar profiles as today, aside from the increased number of vehicles.

The average power demand of the fast charging station was estimated to 4.9 MW per hour during the year. This is a massive increase in the power demand for the grid investigated.

With an initial total average power demand for the whole power grid of approximately 3.6 MW, does this mean an increase in power demand by 136 %. Furthermore, the fast charging station will be responsible for approximately 58 % of the total power demand of the final power grid.

Since the fast charging station is responsible for a significant increase in the total load in the grid will the simulations by the FASaD prototype be significantly affected by the location for this charging station. This is due to the purpose of the simulations performed by the prototype: to minimize the total annual CENS in the system. Verification of how the different locations for the fast charging station will affect the simulations can be seen by the investigation of the different switching sequences for the different locations. For instance, when the additional load is located at substation NS H1 in scenario 1, switches closest to this substation will be opened so that the fast charging station can be resupplied by power rapidly from a reserve connection. Hence, the substation with the absolute highest power demand will have the shortest possible interruption duration for that delivery point. In this way will the total CENS for the power system be minimized.

By simulation of the base load scenario was the annual CENS found to be 156 054 NOK/yr, the interrupted power was 1670.280 kW/yr and the ENS was 3732.206 kWh/yr. From figure 6.2 it is clear that the CENS and the ENS varies some for the different scenarios simulated. The increase in the annual CENS varies from the minimum increase of 236 % in scenario 1 to the maximum increase of 258 % in scenario 2, while the increase in ENS varies from 206 % in scenario 1 to 237 % in scenario 2. Thus, all three scenarios lead to a massive increase in both the CENS and the ENS. Since the purpose of the case study is to find the optimal location will the location with the smallest increase be chosen, regardless of the extent of the increase. It can be found that by choosing location 1, Skagerak Nett can avoid an expense of 33,761 NOK/yr compared to by locating the fast charging station at location 2. Even though this is not a large share of the total CENS, it would be beneficial for grid companies to consider all costs and determine which expenses can be avoided. The increase in interrupted power due to the additional load, which is equal to 176 % for all scenarios, would also be a significant challenge for the power system. In a realistic scenario might none of the locations be chosen without applying several upgrades to the grid, due to this massive increase in CENS and ENS.

For this case study, the most optimal switching sequence will lead to the most optimal fast charging station location as the CENS and the ENS is minimized for this scenario. Thus,

the essential importance of the switching sequence for a power system is a crucial result in this master thesis.

As the criterion for finding the most optimal location is chosen to be the aim of, among other, reducing the total CENS, which is similar to the aim of the FASaD prototype, will this simulation method be appropriate to use. If another criterion was used in the prototype could the results have become very different, with possibly much higher total annual CENS and annual ENS for the power system.

7.2 Impact of a fast charging station at June 29

When the impact of a fast charging station at one specific day is going to be analyzed, the load profile for this day is essential to estimate. The load profile for June 29, the day with the estimated highest power demand, is found by the same justifications and assumptions as the load profile for the whole year. Consequently, the load profile, showed in figure 6.3, have its maximum demand from 1 PM to 9 PM during this day. This means that during these hours will the fast charging station be fully in use, and a queue of vehicles is expected. As the power demand data provided by Skagerak Nett is an average hourly value per year, is the analysis of the 'worst-case' scenario a bit inaccurate. It is reasonable to assume that the power demand of the entire grid will vary significantly during June 29, with a minimum demand during the night and a maximum demand during the day. Hence, the total impact of the varying power demand for the whole system could be more accurate if the input data for all delivery points were given on an hourly basis. However, this would need an enormous quantity of data that must be provided by Skagerak Nett. Since the power demand of the fast charging station is the only demand that varies, this will be the only demand that causes a variation for the reliability indices.

The fault frequency of the components in the grid is also found to perform an hourly analysis of one day. This is obtained from fault statistics by Statnett, where the annual number of faults per hour can be found. Thus, the fault data are not specific for the exact day of the simulations. Additionally, the number of faults is a summation of faults on all components in the grid, and thereby not entirely correct for this simulation as the FASaD prototype only includes faults on some grid components. The inaccuracies following the simplifications done with the input of fault frequencies in the simulations may have some impact on the final results.

By the simulations of the 'worst-case' scenario was the purpose of investigating how the load profile and the fault distribution during a day would impact the reliability of supply in the grid. According to the results by the simulations with the FASaD prototype will the CENS not vary considerably during the day. However, if the costs are corrected by hourly, daily and monthly corrections factors can the variation be detected. Since this is very time-consuming operation can it be concluded with that current input data and the annual examination using the FASaD prototype are not very applicable for finding CENS per hour during one specific day. The variations of the ENS and the interrupted power per hour are much bigger than the variation of CENS. This is mainly found to be because of the massive power demand at the fast charging station, which would cause high interrupted power and further high ENS for this power system.

From the simulations in the FASaD prototype was it found that the variation in fault frequency during a day had minimal impact on the resulting reliability indices. The reason for the lack of impact could be the very low fault frequencies that initially exist for the overhead lines, cables and fault indicators. This includes fault frequencies for both permanent and temporary faults. Most of the fault frequencies range from 10^{-6} to 10^{-2} faults per year for the different components. Thus, small changes in all fault frequencies in the grid, which is done in this case study, will not impact the reliability of this power grid. However, if the fault frequencies were significantly higher might the impact of a change in faults during the day on the total reliability of supply be observed.

To summarize, when using the FASaD prototype to assess one specific day will several simplifications be made. Since the prototype is designed for finding annual reliability indices will this approach in fact set all hours during the year equal to the specific hour that is the intention to simulate. Then, the total annual sum of reliability indices, given that all hours were similar to that specific hour, must be divided by the number of hours in a year. Thus, the approach will not give an utterly realistic result for the case study. Nevertheless, this approach will show interesting trends for the variation of reliability indices during one day.

7.3 Assumptions and limitations

The case study is performed without applying any upgrades to the power grid. In a realistic scenario could this be necessary. Primarily, when a new fast charging station is developed,

will this almost always require the installation of a new substation. This is because of the significant high power demand needed by the fast charging station. With an increase of 136 % in the power demand in the grid due to the fast charging station, may this require an upgrade of the transformer. If the current transformer can manage this massive increase, it would mean that with the initial load would the transformer be oversized. This is not analyzed in this master thesis. Furthermore, in the FASaD prototype is it assumed that reserve connections will be able to supply the required power to some parts of the power grid during a fault. For this case study will the fast charging station require a significant power demand, which in reality may be challenging to supply from a reserve connection if the quality of supply should be according to the regulations in FASIT.

The power cable or overhead line that must be developed from the existing grid to the new charging station is assumed to be very short, thus will this cable not contribute to increasing the reliability indices considerably. In a realistic scenario will the new substation that should be built lead to the development of a cable or an overhead line that will have a fault frequency which must be taken into account. Further, the fast charging station could lead to an overload of the cables and overhead lines upstream the load point, and thereby a higher fault frequency for these cables as well.

The variation in charging time of EVs during a year, and its impact on the length of the charging queue, is not taken into consideration in the case study. As table 4.4 shows will the ambient temperature have an impact on the charging time, which could be modelled in the simulation. However, as the variation probably will have a small impact on the total reliability of supply is this chosen to be neglected. The neglect of the variation in charging time could additionally be justified as there will be the longest queues during summer, which can be seen from figure 5.3. The months that usually are the coldest are also the months with the minimum traffic at E18 during a year. As the ambient temperature during winter will require a longer time of charging, will this not cause significant long queues since the number of vehicles at the station is significantly smaller than during the summer. As [23] presents, 50 % of all EV owners accept a waiting time of 20 minutes at the charging stations. Hence, the assumptions of utilizing all the power at the fast charging station at many hours during the day might be a small misrepresentation of a realistic scenario. It is assumed that vehicles will wait until a charger is available, and this might be longer than 20 minutes. For road freight transport is it assumed that the charging will happen during the required break for the driver, and thereby is it assumed that the drivers are willing to wait for a more extended period than the EV owners.

The decision of choosing the alternative locations for the fast charging station is based on the distance to E18 and the grid, and on the basis that all locations have some distance between each other, to illustrate the location's impact of the reliability of supply. Thus, chosen locations are located at different sites in the grid for illustration of the importance of correct location in order to minimize the impact of reliability of supply in the power grid. As other circumstances when choosing the location must be taken into consideration, will this be a simplified illustration. A more realistic scenario requires a thorough analysis of the locations. Among others, the location must be accepted by the current landowners and the topography of the area must be considered appropriate for a fast charging station.

In this master thesis have only a small part of the impact a charging station will have on the quality of supply been investigated. To accurate find the total impact of a charging station must all aspects of the power system be measured. A problem that probably will cause challenges if the fast charging station was developed will be harmonics. Harmonics is a concern in the quality of supply that is not considered in this master thesis. If a fast charging station was proposed to be connected to the grid in Sande must Skagerak Nett perform necessary calculations and studies regarding all concerns of quality of supply.

The case study in this master thesis is performed on one of the real power grids in Sande. Even though the results primarily would apply for this grid, could the principles be applied for other grids as well. Among others, the fast charging station's distance to the transformer and reserve connections will be significant for the reliability of supply in the power system. For other power systems will the grid topography and grid parameters be different, which can lead to an optimal location elsewhere in the grid. It is found that by using the FASaD prototype will the large loads in a grid be prioritized in regards to minimizing the interruption duration at these load points. In this power grid is the fast charging station definitely the largest load in the system. For other grids may this not be the situation, and the switching sequence may not be in favour of the fast charging station.

Chapter 8

Conclusion

The reliability of supply in a power system will be affected if a fast charging station is connected to the system. By simulations using the FASaD prototype, it has been found that the fast charging station's location relative to the transformer and the reserve connections in a power grid will have an impact on the reliability of supply. It is found that the most optimal location in the examined grid is a delivery point located some distance downstream from the circuit breaker and very close to a reserve connection. The location closest to the transformer was the second-best option, while the location further downstream the grid was the least optimal alternative. However, all three examined alternative locations led to a massive increase in the reliability indices. The increase was 176% for the annual interrupted power, there was a 236 % - 258 % increase in the annual CENS and a 206 % - 237 % increase in the annual ENS for the different scenarios.

The case study showed that the switching sequence during a fault is important for, among others, minimizing the total annual CENS in the grid. The location for the fast charging station that led to a switching sequence that minimized the CENS the most, was found to be the most optimal. Reliability analyzes using the FASaD prototype is beneficial when the aim of the simulation is to minimize the total CENS in the power grid. For a grid where the fast charging station has the highest power demand could the optimal switching sequence lead to a relatively quick resupply of power to the fast charging station in order to minimize the CENS.

By reliability analyzes of the day with the estimated maximum power demand, it was found that the change in the fault frequency during the day will have minimal impact on

the reliability of supply of this power system. Investigation showed that the interrupted power and the ENS of the entire grid during the day would depend strongly on the load profile of the fast charging station. Further, it was shown that the FASaD prototype found a minimal variation in CENS per hour. However, if corrections are performed manually for hourly, daily, and monthly specific costs at all delivery points could a variation of CENS be detected.

Chapter 9

Further work

This master thesis shows an alternative way of finding the load profile of a fast charging station, which would give an estimation that can be used for further reliability analyzes. A method for accurate estimation of future load profiles for fast charging stations should be developed for further analyses. This could be advantageous for, among others, grid companies who will get an improved overview of the varying massive power demand from the large fast charging stations. A complete analysis of future power demand for fast charging of vehicles should, among others, include political aspects such as incentives for purchasing EVs and pricing of electricity at the charging station. Additionally could a precise prediction of vehicles passing a specific location along the roads in the future be beneficial to find. Thus, this comprehensive investigation could be done a separate master thesis.

Reliability of supply has been the primary focus of this case study. Only one real grid has been examined, and further work could, therefore, consist of the investigation of several grids. In order to fully assess the impact a charging station will have on the power grid must all aspects of the quality of supply be investigated. Hence, an extensive study must be performed. Additionally, it will be essential to perform a power-flow analysis to simulate an even more realistic scenario.

Chapter 10

Bibliography

[1] SINTEF Energi AS. Planleggingsbok for kraftnett, 2010.

[2] Marte Røine Brurås. Impact of electric vehicles on the reliability of electricity supply in distribution networks. Project Work, December 2018.

[3] Elbilforening. Ionity åpner første lynlader med 350 kw. https://elbil.no/ionity-apner-forste-lynlader-med-350-kw/, February 2019.

[4] Elbilforeningen. Elbilbestand. https://elbil.no/elbilstatistikk/elbilbestand/, December 18.

[5] Elbilforeningen. Ladeklart norge 2025, March 2019.

[6] Elbilforeningen. Ladestasjoner. https://elbil.no/lading/ladestasjoner/, April 2019.

[7] Elbilforeningen. Slik får du hurtigst mulig lading i kulda. https://elbil.no/slik-far-du-hurtigst-mulig-lading-i-kulda/, April 2019.

[8] Electrive. Tesla superchargers charging with a power up to 150 kw. https://www.electrive.com/2019/04/27/tesla-superchargers-charge-capacity-up-to-150-kw/, April 2019.

[9] Electrive. Vehicle manufactures renault, nissan and mitsubishi want solid-state batteries. https://www.electrive.com/2018/03/12/renault-nissan-mitsubishi-wants-solid-state-batteries-by-2025/, March 2019.

[10] entsoe. Nordic and baltic grid disturbance statistics 2017. https://www.fingrid.fi/globalassets/dokumentit/fi/kantaverkko/suomen-sahkojarjestelma/hvac2017$finalkotisivuille.pdf$, 2018.

[11] Eurelectric. Electrification of heavy duty vehicles in the future. https://www.eurelectric.org/media/2161/electrification$ofheavydutyvehicles-2017-030-0588$

[12] Hans Faanes and Arne Holen. Kompendium tfe4112 - elforsyning - del 1. Kompendium, NTNU, February 2015.

[13] FASIT. Feil og avbrudd i kraftsystemet. http://fasit.nsp01cp.nhosp.no/generelle-krav/category237.html, January 2011.

[14] Fastned. Everything you've always wanted to know about fast charging. https://fastned.nl/en/blog/post/everything-you-ve-always-wanted-to-know-about-fast-charging, May 2018.

[15] Fjordkraft. Ladestasjoner i norge. https://www.ladestasjoner.no/kart/, April 2019.

[16] SINTEF Energy Research Gerd Kjølle. The cost of energy not supplied arrangement (cens). https://www.sintef.no/globalassets/project/kile$uk/the-cost-of-energy-not-supplied-arrangement.pdf, April$2009.

[17] MAN Truck Germany. Man e-truck. https://www.truck.man.eu/de/en/man-etruck.html, April 2019.

[18] Håvard Hansen, Eirik Eggum, Astrid Ånestad, and C Aabakken. Avbrotsstatistikk 2017. *Norges vassdrags-og energidirektorat, Tech. Rep*, (43-2017):2017, 2018.

[19] Tonje Hermansen, Hanne Vefsnmo, and Håkon Marthinsen. Prosjektnotat - fasad metodikk for pålitelighetsanalyse av distribusjonsnett, December 2018.

[20] Tonje Hermansen, Hanne Vefsnomo, Gerd Kjølle, Kjell Anders Tutvedt, and Stig Simonsen. Reliability analysis methodology for smart fault handling in mv distribution grids. *CIRED*, 2019.

[21] IEC. Definision of reliability. http://www.electropedia.org/iev/iev.nsf/display?openform&ievref=6 01-01, November 18.

[22] IEC. Power system faults. http://www.electropedia.org/iev/iev.nsf/display?openform&ievref=448- 13-02, 2019.

[23] Norwegian Centre for Transport Research Institute of Transport Economics. Charging into the future - analysis of fast charger use, 2019.

[24] Md Shariful Islam and N Mithulananthan. Daily ev load profile of an ev charging station at business premises. In *Innovative Smart Grid Technologies-Asia (ISGT-Asia), 2016 IEEE*, pages 787–792. IEEE, 2016.

[25] SINTEF Energiforskning As Kjell Sand. Arbeidsnotat - leveringskvalitet - en oversikt, 2008.

[26] Gerd Kjølle and Oddbjørn Gjerde. The opal methodology for reliability analysis of power systems. *SINTEF Energy Research, Trondheim, Norway, Tech. Rep. A-7175*, 2012.

[27] Gerd Kjolle and Kjell Sand. Relrad-an analytical approach for distribution system reliability assessment. *IEEE Transactions on Power Delivery*, 7(2):809–814, 1992.

[28] Gerd Kjølle. Prosjektnotat - kile-satsene og hva de dekker. https://www.sintef.no/globalassets/project/kile/prosjektnotat$kile - satserv42011 - 01 - 20.pdf, January2011$.

[29] Gerd Kjølle. Elk10 quality of supply in electrical power systems - power system reliability/reliability of supply, November 2018.

[30] Prabha Kundur, John Paserba, Venkat Ajjarapu, Göran Andersson, Anjan Bose, Claudio Canizares, Nikos Hatziargyriou, David Hill, Alex Stankovic, Carson Taylor, et al. Definition and classification of power system stability. *IEEE transactions on Power Systems*, 19(2):1387–1401, 2004.

[31] Oluf Langhelle and Rolf Bohne. Electric roads in norway? - summary of a concept analysis, September 2018.

[32] Transport & Mobility Leuven and IRU contribution. Commercial vehicleof the future - a roadmap towards fully sustainable truck operations. Technical report, Transport & Mobility Leuven, 2017.

[33] Mary Ann Lundteigen and Marvin Rausand. Relaibility block diagrams (rbd). https://www.ntnu.edu/documents/624876/1277046207/SIS+book+-+chapter+05+-+Introduction+to+RBDs/61af88f9-b6d6-402a-94f7-902706c921c7, May 2019.

[34] Miljøstatus. Emissions from transport. http://www.miljostatus.no/tema/klima/norske-klimagassutslipp/utslipp-av-klimagasser-fra-transport/, January 2018.

[35] Doros Nicolaides, David Cebon, and John Miles. Prospects for electrification of road freight. *IEEE Systems Journal*, 12(2):1838–1849, 2017.

[36] Energy Facts Norway. The electricity grid. https://energifaktanorge.no/en/norsk-energiforsyning/kraftnett/, May 2019.

[37] NVE. Kart over nettanlegg - sande. https://temakart.nve.no/link/?link=nettanlegg, April 19.

[38] NVE. Development in transport sector. https://www.nve.no/energy-consumption-and-efficiency/energy-consumption-in-norway/development-in-the-transport-sector/, October 2018.

[39] NVE. Economic regulation. https://www.nve.no/energy-market-and-regulation/economic-regulation/, May 2018.

[40] NVE. The norwegian power system - grid connection and licensing. https://www.statkraftdatacentersites.com/globalassets/9-statkraft-datacentres/documents/faktaark-energi-nve.pdf, August 2018.

[41] NVE. About nve norwegian contact information network tariffs. https://www.nve.no/energy-market-and-regulation/network-regulation/network-tariffs/, May 2019.

[42] OECD/IEA. Nordicevoutlook2018 - insights from leaders in electric mobility, 2018.

[43] Olje og Energi Departementet. Forskrift om økonomisk og teknisk rapportering, inntektsramme for nettvirksomheten og tariffer, April 2.

[44] Olje og Energidepartementet. Forskrift om leveringskvalitet i kraftsystemet, 2004.

[45] Klima og Miljødepertamentet. Statsbudsjettet 2019. https://www.statsbudsjettet.no/Statsbudsjettet-2019/Dokumenter1/Fagdepartementenes-proposisjoner/klima-Miljo/Prop-1-S-/Del-4-Rapportering-etter-Lov-om-klimamal–klimalova-/12-Klimamal-mot-2030-og-2050-og-Noregs-karbonbudsjett-/, April 2019.

[46] Electric Revs. How to supercharge a tesla semi. https://electricrevs.com/2019/02/15/how-to-supercharge-a-tesla-semi/, May 2019.

[47] Knut Samdal, GH Kjolle, Balbir Singh, and O Kvitastein. Interruption costs and consumer valuation of reliability of service in a liberalised power market. In *2006 International Conference on Probabilistic Methods Applied to Power Systems*, pages 1–7. IEEE, 2006.

[48] Samferdselsdepartamentet. Nasjonal transportplan 2019-2029, 2016-2017.

[49] Kjell Sand. What is quality of supply, 2018.

[50] Pernille Berbu Seth. Selvhelende distribusjonsnett ved bruk av feilindikatorer og fjernstyring. Master's thesis, Norges teknisk-naturvitenskapelige universitet, 2018.

[51] Christer H Skotland, Eirik Eggum, and Dag Spilde. Hva betyr elbiler for strømnettet? *NVE Rapport nr 74*, 2016.

[52] Dag Spilde and Christer Skotland. Hvordan vil en omfat-tende elektrifisering av transportsektoren pvirke kraftsystemet? *NVE, Oslo, Norway, Tech. Rep.*, 2015.

[53] Statnett. Årsstatistikk 2017 - driftsforstyrrelser, feil og planlagte utkoplinger i 1-22 kv-nettet, September 2018.

[54] Tesla. Tesla semi. $https://www.tesla.com/noNO/semi?redirect=no$, May 2019.

[55] Statens vegvesen Tom E. Nørbech. Tungtrafkkprognoser pa utvalgte veger. https://www.vegvesen.no/$attachment$/2322574/$binary$/1261782?$fasttitle = Rapport + 6 + - + 7$

[56] Kjell Anders Tutvedt, Robert Seguin, Gerd Kjølle, Stig Simonsen, Tonje Skoglund Hermansen, and Ingrid Myhr. Smart fault handling in medium-voltage distribution grids. *CIRED-Open Access Proceedings Journal*, 2017(1):1471–1474, 2017.

[57] Hanne Vefsnmo, Håkon Mathinsen, and Tonje Hermansen. Prosjektnotat - brukerveiledning fasad-prototypen, November 2018.

[58] Statens Vegvesen. Adt for bolstad tunnel. https://www.vegvesen.no/trafikkdata/start/utforsk?data April 2019.

[59] Statens Vegvesen. Batteri til elbil. https://www.vegvesen.no/kjoretoy/Eie+og+vedlikeholde/elkjor April 2019.

Appendix A

Appendix

Hour	**Jan**	**Feb**	**Mar**	**Apr**	**May**	**Jun**	**Jul**	**Aug**	**Sept**	**Oct**	**Nov**	**Dec**
1	0,967	1,042	1,080	1,230	1,387	1,545	1,586	1,438	1,336	1,248	0,989	1,074
2	0,612	0,660	0,684	0,779	0,879	0,978	1,004	0,911	0,846	0,790	0,626	0,680
3	0,442	0,477	0,495	0,563	0,635	0,707	0,726	0,658	0,612	0,571	0,453	0,492
4	0,521	0,562	0,583	0,663	0,748	0,833	0,855	0,775	0,721	0,673	0,533	0,579
5	0,467	0,503	0,522	0,594	0,670	0,746	0,766	0,694	0,645	0,602	0,477	0,518
6	1,394	1,502	1,558	1,774	2,001	2,227	2,287	2,074	1,927	1,799	1,426	1,549
7	3,015	3,249	3,370	3,837	4,328	4,818	4,947	4,486	4,168	3,891	3,084	3,350
8	3,333	3,592	3,726	4,242	4,784	5,326	5,469	4,960	4,608	4,302	3,410	3,703
9	3,781	4,076	4,227	4,813	5,428	6,043	6,205	5,627	5,228	4,881	3,869	4,202
10	4,296	4,631	4,803	5,469	6,168	6,866	7,051	6,393	5,940	5,546	4,396	4,774
11	5,617	6,055	6,280	7,150	8,064	8,977	9,218	8,359	7,767	7,251	5,747	6,242
12	6,751	7,276	7,546	8,593	9,691	10,00	10,00	10,00	9,333	8,713	6,907	7,501
13	6,441	6,943	7,201	8,199	9,247	10,00	10,00	9,585	8,906	8,315	6,590	7,158
14	6,717	7,240	7,509	8,550	9,643	10,00	10,00	9,996	9,287	8,670	6,872	7,464
15	6,757	7,282	7,553	8,600	9,699	10,00	10,00	10,00	9,342	8,721	6,913	7,508
16	7,617	8,210	8,515	9,696	10,00	10,00	10,00	10,00	10,00	9,832	7,793	8,464
17	7,320	7,890	8,183	9,318	10,00	10,00	10,00	10,00	10,00	9,449	7,489	8,134
18	6,708	7,230	7,499	8,539	9,630	10,00	10,00	9,982	9,275	8,659	6,863	7,454
19	5,717	6,162	6,391	7,277	8,207	9,137	9,382	8,508	7,905	7,380	5,850	6,353
20	4,899	5,281	5,477	6,236	7,033	7,829	8,040	7,291	6,774	6,324	5,013	5,444
21	3,439	3,707	3,844	4,377	4,937	5,496	5,643	5,117	4,755	4,439	3,518	3,821
22	3,230	3,481	3,611	4,111	4,637	5,161	5,300	4,806	4,466	4,169	3,304	3,589
23	2,285	2,462	2,554	2,908	3,279	3,651	3,749	3,400	3,159	2,949	2,337	2,539
24	1,754	1,891	1,961	2,233	2,518	2,803	2,879	2,611	2,426	2,264	1,795	1,949

Table A.1: Demand [MWh/h] for weekdays

Hour	**Jan**	**Feb**	**Mar**	**Apr**	**May**	**Jun**	**Jul**	**Aug**	**Sep**	**Oct**	**Nov**	**Dec**
1	0,843	0,908	0,942	1,072	1,209	1,346	1,383	1,254	1,165	1,088	0,862	0,936
2	0,679	0,732	0,759	0,864	0,974	1,085	1,114	1,010	0,938	0,876	0,694	0,754
3	0,568	0,612	0,635	0,723	0,815	0,907	0,932	0,845	0,785	0,733	0,581	0,631
4	0,919	0,991	1,027	1,170	1,319	1,469	1,508	1,368	1,271	1,186	0,940	1,021
5	0,454	0,490	0,508	0,578	0,652	0,726	0,745	0,676	0,628	0,586	0,465	0,505
6	0,652	0,703	0,729	0,830	0,936	1,043	1,071	0,971	0,902	0,842	0,667	0,725
7	0,634	0,683	0,709	0,807	0,910	1,013	1,040	0,943	0,876	0,818	0,649	0,704
8	0,660	0,712	0,738	0,840	0,948	1,055	1,084	0,983	0,913	0,852	0,676	0,734
9	1,170	1,261	1,308	1,489	1,680	1,870	1,920	1,741	1,618	1,510	1,197	1,300
10	2,063	2,223	2,306	2,626	2,961	3,296	3,385	3,070	2,852	2,663	2,110	2,292
11	3,587	3,866	4,010	4,565	5,149	5,732	5,886	5,337	4,959	4,630	3,670	3,985
12	5,634	6,072	6,298	7,171	8,087	9,003	9,245	8,383	7,789	7,272	5,764	6,260
13	7,089	7,641	7,925	9,023	10,00	10,00	10,00	10,00	9,801	9,150	7,253	7,877
14	7,617	8,210	8,515	9,696	10,00	10,00	10,00	10,00	10,00	9,832	7,793	8,464
15	7,614	8,207	8,512	9,692	10,00	10,00	10,00	10,00	10,00	9,829	7,790	8,461
16	7,237	7,800	8,090	9,212	10,00	10,00	10,00	10,00	10,00	9,341	7,404	8,041
17	6,870	7,404	7,680	8,744	9,862	10,00	10,00	10,00	9,498	8,867	7,028	7,633
18	7,453	8,033	8,332	9,487	10,00	10,00	10,00	10,00	10,00	9,621	7,626	8,282
19	6,875	7,410	7,686	8,751	9,869	10,00	10,00	10,00	9,505	8,874	7,034	7,639
20	6,613	7,128	7,393	8,418	9,494	10,00	10,00	9,841	9,144	8,537	6,766	7,349
21	5,998	6,465	6,705	7,635	8,610	9,585	9,843	8,926	8,293	7,742	6,137	6,665
22	5,103	5,500	5,704	6,495	7,325	8,154	8,374	7,593	7,055	6,586	5,221	5,670
23	3,558	3,835	3,977	4,528	5,107	5,685	5,838	5,294	4,919	4,592	3,640	3,953
24	0,203	0,219	0,227	0,259	0,292	0,325	0,334	0,303	0,281	0,263	0,208	0,226

Table A.2: Demand [MWh/h] for weekends

Name	**Annual number of partial interruptions [/yr]**	**Average interruption duration [min/interruption]**	**Annual interruption duration [min/yr]**	**Annual interruption cost [NOK/yr]**	**Annual number of interruptions [/yr]**	**Annual interrupted power [kW/yr]**	**Annual energy not supplied [kWh/yr]**
NS A2	1,894	91,472	84,938	888,999	0,601	15,428	36,330
NS H4	1,197	103,517	96,123	1842,755	0,601	25,096	66,878
NS L1	0,897	94,133	87,409	659,950	0,601	10,099	24,474
NS I3	1,154	97,436	90,475	0,000	0,601	0,000	0,000
NS I1	1,154	95,787	88,945	7080,378	0,601	54,600	134,638
NS K3	0,929	93,809	87,108	920,743	0,601	16,723	40,385
NS K2	0,957	102,332	95,022	581,989	0,601	10,541	27,769
NS M1	0,784	99,460	92,356	2471,102	0,601	24,061	61,606
NS L3	0,814	94,503	87,753	4212,643	0,601	60,142	146,318
NS C3	1,882	80,177	74,450	5170,925	0,601	38,120	78,682
NS G2	1,291	108,678	100,915	1758,177	0,601	26,298	73,577
NS H3	1,197	103,517	96,123	1613,414	0,601	24,244	64,609
NS H2	1,197	91,410	84,880	838,110	0,601	16,635	39,146
NS H6	1,169	92,168	85,584	2837,175	0,601	22,838	54,188
NS M4	0,784	101,969	94,686	482,041	0,601	8,795	23,087
NS I2	1,154	98,020	91,018	1771,652	0,601	28,082	70,863
NS C1	1,886	80,121	74,398	18773,813	0,601	278,787	575,026
NS C2	1,886	81,067	75,276	12202,693	0,601	181,485	378,750
NS B2	1,927	90,397	83,940	1154,147	0,634	13,759	30,338
NS L5	0,814	95,847	89,001	1641,793	0,601	31,724	78,278
NS D1	1,878	84,759	78,705	2094,765	0,601	37,772	82,419
NS E3	1,730	88,747	82,408	0,000	0,601	0,000	0,000
NS M2	0,784	94,765	87,996	1927,264	0,601	12,860	31,372
NS M3	0,784	101,969	94,686	1524,512	0,601	10,672	28,014
NS H5	1,197	103,517	96,123	1745,266	0,601	13,208	35,199
NS J3	1,017	106,737	99,113	1397,052	0,601	6,076	16,695
NS H1	1,201	91,335	84,811	5595,247	0,601	19,467	45,772
NS K1	0,957	93,699	87,006	3049,464	0,601	18,008	43,437
NS F1	1,730	82,156	76,287	87,203	0,601	0,511	1,080
NS F3	1,325	103,843	96,425	3383,087	0,601	7,448	19,912
NS F4	1,307	103,910	96,488	0,103	0,601	0,000	0,001
NS F5	1,276	89,837	83,419	3602,423	0,601	17,884	41,361
NS E2	1,730	88,747	82,408	2960,557	0,601	23,831	54,446
NS F2	1,325	88,569	82,242	185,406	0,601	0,924	2,107
NS E1	1,710	82,453	76,563	139,068	0,601	55,587	117,991
NS E4	1,690	82,816	76,900	19201,460	0,601	95,769	204,177
NS J1	1,012	106,744	99,119	640,614	0,601	9,375	25,763
NS J2	1,012	108,103	100,381	518,829	0,601	7,840	21,819
NS A1	1,894	91,472	84,938	41,629	0,601	0,556	1,309
NS G1	1,291	108,240	100,508	2600,905	0,601	5,511	15,356
NS L2	0,828	94,346	87,606	3260,974	0,601	62,877	152,716
NS E7	1,947	98,865	91,803	8998,440	0,879	28,245	49,138
NS E6	1,684	87,994	81,708	122,341	0,617	2,451	5,411
NS E5	1,669	83,204	77,261	1019,275	0,601	5,079	10,878
NS L4	0,804	94,647	87,887	2180,424	0,601	29,476	71,820
NS D2	1,878	80,362	74,622	596,608	0,601	7,449	15,411
NS B1	1,927	87,117	80,894	455,209	0,634	7,152	15,197

Table A.3: Reliability indices for every delivery point - Base Load Scenario

Name	Annual number of partial interruptions [/yr]	Average interruption duration [min/interruption]	Annual interruption duration [min/yr]	Annual number of interruptions [/yr]	Annual interruption cost [NOK/yr]	Annual interrupted power [kW/yr]	Annual energy not supplied [kWh/yr]
NS A2	1,890	87,886	81,608	0,601	831,486	15,428	34,906
NS H4	1,197	96,591	89,691	0,601	1735,933	25,096	62,404
NS L1	0,968	86,817	80,616	0,601	615,735	10,099	22,572
NS I3	1,154	90,509	84,044	0,601	0,000	0,000	0,000
NS I1	1,154	88,861	82,513	0,601	6734,354	54,600	124,902
NS K3	1,000	86,493	80,315	0,601	858,138	16,723	37,236
NS K2	1,028	95,017	88,230	0,601	544,518	10,541	25,784
NS M1	0,855	92,145	85,563	0,601	2331,475	24,061	57,075
NS L3	0,885	87,188	80,960	0,601	3945,769	60,142	134,991
NS C3	1,878	76,591	71,120	0,601	4880,266	38,120	75,163
NS G2	1,546	101,435	94,189	0,601	1653,939	26,298	68,673
NS H3	1,197	96,591	89,691	0,601	1518,381	24,244	60,286
NS H2	1,197	84,483	78,449	0,601	778,977	16,635	36,180
NS H6	1,169	85,242	79,153	0,601	2676,472	22,838	50,116
NS M4	0,855	94,654	87,893	0,601	450,778	8,795	21,431
NS I2	1,154	91,094	84,586	0,601	1661,889	28,082	65,855
NS C1	1,882	76,535	71,068	0,601	17451,505	278,787	549,292
NS C2	1,882	77,481	71,947	0,601	11350,560	181,485	361,998
NS B2	1,923	86,812	80,610	0,634	1082,693	13,759	29,135
NS L5	0,885	88,532	82,208	0,601	1529,020	31,724	72,303
NS D1	1,874	81,174	75,375	0,601	1960,850	37,772	78,932
NS E3	1,726	85,162	79,078	0,601	0,000	0,000	0,000
NS M2	0,855	87,450	81,203	0,601	1856,068	12,860	28,950
NS M3	0,855	94,654	87,893	0,601	1476,642	10,672	26,004
NS H5	1,197	96,591	89,691	0,601	1649,997	13,208	32,843
NS J3	1,088	99,422	92,320	0,601	1324,250	6,076	15,551
NS H1	1,272	84,020	78,018	0,601	383272,936	2965,172	6413,572
NS K1	1,028	86,383	80,213	0,601	2967,831	18,008	40,046
NS F1	1,726	78,570	72,958	0,601	82,921	0,511	1,033
NS F3	1,579	96,600	89,700	0,601	3229,253	7,448	18,523
NS F4	1,562	96,667	89,762	0,601	0,101	0,000	0,001
NS F5	1,530	82,593	76,693	0,601	3516,804	17,884	38,026
NS E2	1,726	85,162	79,078	0,601	2779,302	23,831	52,247
NS F2	1,579	81,325	75,516	0,601	180,981	0,924	1,935
NS E1	1,706	78,867	73,233	0,601	135,653	55,587	112,860
NS E4	1,685	79,230	73,570	0,601	18742,976	95,769	195,336
NS J1	1,083	99,428	92,326	0,601	602,453	9,375	23,998
NS J2	1,083	100,787	93,588	0,601	488,010	7,840	20,342
NS A1	1,890	87,886	81,608	0,601	38,963	0,556	1,258
NS G1	1,546	100,997	93,782	0,601	2486,261	5,511	14,329
NS L2	0,899	87,030	80,813	0,601	3038,061	62,877	140,875
NS E7	1,943	95,280	88,473	0,879	8609,216	28,245	47,356
NS E6	1,680	84,408	78,379	0,617	114,677	2,451	5,190
NS E5	1,665	79,618	73,931	0,601	994,962	5,079	10,409
NS L4	0,875	87,332	81,094	0,601	2045,864	29,476	66,269
NS D2	1,874	76,776	71,292	0,601	570,185	7,449	14,723
NS B1	1,923	83,531	77,565	0,634	425,127	7,152	14,571

Table A.4: Reliability indices for every delivery point - Scenario 1

Name	Annual number of partial interruptions [/yr]	Average interruption duration [min/interruption]	Annual interruption duration [min/yr]	Annual number of interruptions [/yr]	Annual interruption cost [NOK/yr]	Annual interrupted power [kW/yr]	Annual energy not supplied [kWh/yr]
NS A2	1,852	93,814	87,112	0,601	890,929	15,428	37,260
NS H4	1,156	104,379	96,923	0,601	1846,129	25,096	67,435
NS L1	0,838	94,381	87,639	0,601	661,056	10,099	24,539
NS I3	1,113	98,297	91,276	0,601	0,000	0,000	0,000
NS I1	1,113	96,649	89,745	0,601	7091,375	54,600	135,849
NS K3	0,939	93,765	87,067	0,601	404013,873	2962,428	7150,851
NS K2	1,032	102,228	94,926	0,601	582,926	10,541	27,741
NS M1	0,784	99,634	92,517	0,601	2468,323	24,061	61,714
NS L3	0,814	94,677	87,914	0,601	4219,322	60,142	146,586
NS C3	1,840	82,519	76,624	0,601	5178,199	38,120	80,980
NS G2	1,341	109,728	101,890	0,601	1760,582	26,298	74,288
NS H3	1,156	104,379	96,923	0,601	1615,523	24,244	65,147
NS H2	1,156	92,271	85,680	0,601	839,946	16,635	39,515
NS H6	1,128	93,030	86,385	0,601	2841,197	22,838	54,694
NS M4	0,784	102,143	94,847	0,601	482,823	8,795	23,126
NS I2	1,113	98,881	91,818	0,601	1774,666	28,082	71,486
NS C1	1,844	82,463	76,572	0,601	18806,903	278,787	591,832
NS C2	1,844	83,409	77,450	0,601	12223,362	181,485	389,691
NS B2	1,885	92,739	86,114	0,634	1155,935	13,759	31,124
NS L5	0,814	96,020	89,161	0,601	1644,614	31,724	78,420
NS D1	1,835	87,101	80,879	0,601	2098,332	37,772	84,696
NS E3	1,688	91,089	84,582	0,601	0,000	0,000	0,000
NS M2	0,784	94,939	88,157	0,601	1929,045	12,860	31,430
NS M3	0,784	102,143	94,847	0,601	1519,468	10,672	28,061
NS H5	1,156	104,379	96,923	0,601	1746,037	13,208	35,492
NS J3	1,069	106,663	99,044	0,601	1401,020	6,076	16,683
NS H1	1,160	92,197	85,611	0,601	5601,644	19,467	46,204
NS K1	1,032	93,595	86,909	0,601	3051,507	18,008	43,389
NS F1	1,688	84,497	78,462	0,601	87,311	0,511	1,111
NS F3	1,375	104,893	97,401	0,601	3392,304	7,448	20,113
NS F4	1,357	104,960	97,463	0,601	0,104	0,000	0,001
NS F5	1,326	90,887	84,394	0,601	3604,566	17,884	41,845
NS E2	1,688	91,089	84,582	0,601	2962,050	23,831	55,883
NS F2	1,375	89,619	83,217	0,601	185,516	0,924	2,132
NS E1	1,668	84,795	78,737	0,601	139,154	55,587	121,342
NS E4	1,647	85,157	79,074	0,601	19212,933	95,769	209,950
NS J1	1,064	106,669	99,050	0,601	641,796	9,375	25,745
NS J2	1,064	108,028	100,311	0,601	519,495	7,840	21,804
NS A1	1,852	93,814	87,112	0,601	41,669	0,556	1,343
NS G1	1,341	109,290	101,483	0,601	2608,950	5,511	15,505
NS L2	0,828	94,519	87,767	0,601	3266,552	62,877	152,997
NS E7	1,905	101,207	93,977	0,879	9008,180	28,245	50,302
NS E6	1,642	90,335	83,882	0,617	123,309	2,451	5,555
NS E5	1,626	85,546	79,435	0,601	1019,884	5,079	11,184
NS L4	0,804	94,821	88,048	0,601	2183,791	29,476	71,952
NS D2	1,835	82,704	76,796	0,601	597,269	7,449	15,860
NS B1	1,885	89,459	83,069	0,634	455,960	7,152	15,605

Table A.5: Reliability indices for every delivery point - Scenario 2

Name	Average interruption duration [min/interruption]	Annual number of partial interruptions [/yr]	Annual interruption duration [min/yr]	Annual number of interruptions [/yr]	Annual interruption cost [NOK/yr]	Annual interrupted power [kW/yr]	Annual energy not supplied [kWh/yr]
NS A2	94,450	1,879	87,703	0,601	891,566	15,428	37,513
NS H4	104,006	1,177	96,576	0,601	1842,071	25,096	67,194
NS L1	93,483	1,005	86,805	0,601	659,572	10,099	24,305
NS I3	97,924	1,134	90,929	0,601	0,000	0,000	0,000
NS I1	96,275	1,134	89,398	0,601	7078,185	54,600	135,324
NS K3	93,158	1,036	86,504	0,601	920,208	16,723	40,105
NS K2	101,682	1,064	94,419	0,601	581,668	10,541	27,593
NS M1	98,810	0,891	91,752	0,601	2468,504	24,061	61,204
NS L3	93,853	0,921	87,149	0,601	4210,362	60,142	145,311
NS C3	83,155	1,867	77,215	0,601	5168,440	38,120	81,604
NS G2	107,441	1,526	99,766	0,601	1756,382	26,298	72,739
NS H3	104,006	1,177	96,576	0,601	1612,513	24,244	64,914
NS H2	91,898	1,177	85,334	0,601	837,960	16,635	39,355
NS H6	92,657	1,149	86,038	0,601	2835,801	22,838	54,475
NS M4	101,319	0,891	94,082	0,601	481,774	8,795	22,940
NS I2	98,508	1,134	91,471	0,601	1770,801	28,082	71,216
NS C1	83,099	1,871	77,163	0,601	18762,508	278,787	596,396
NS C2	84,044	1,871	78,041	0,601	12194,976	181,485	392,661
NS B2	93,375	1,912	86,705	0,634	1153,536	13,759	31,337
NS L5	95,197	0,921	88,397	0,601	1640,828	31,724	77,747
NS D1	87,737	1,862	81,470	0,601	2093,755	37,772	85,314
NS E3	92,493	1,630	85,886	0,601	0,000	0,000	0,000
NS M2	94,115	0,891	87,392	0,601	1926,655	12,860	31,157
NS M3	101,319	0,891	94,082	0,601	1522,705	10,672	27,835
NS H5	104,006	1,177	96,576	0,601	1743,924	13,208	35,365
NS J3	105,541	1,194	98,002	0,601	1392,394	6,076	16,508
NS H1	91,409	1,248	84,880	0,601	5593,061	19,467	45,809
NS K1	93,049	1,064	86,402	0,601	3048,766	18,008	43,135
NS F1	85,901	1,630	79,765	0,601	87,167	0,511	1,129
NS F3	102,606	1,559	95,277	0,601	3405,533	7,448	19,675
NS F4	102,673	1,542	95,339	0,601	0,104	0,000	0,001
NS F5	88,538	1,559	82,214	0,601	3601,691	17,884	40,763
NS E2	92,493	1,630	85,886	0,601	2955,557	23,831	56,744
NS F2	87,331	1,559	81,093	0,601	185,368	0,924	2,078
NS E1	86,225	1,589	80,065	0,601	385952,286	3001,292	6662,062
NS E4	86,738	1,549	80,542	0,601	19197,540	95,769	213,847
NS J1	105,547	1,189	98,008	0,601	639,860	9,375	25,474
NS J2	106,906	1,189	99,269	0,601	518,764	7,840	21,577
NS A1	94,450	1,879	87,703	0,601	41,589	0,556	1,352
NS G1	107,003	1,526	99,359	0,601	2622,840	5,511	15,181
NS L1	93,696	0,935	87,003	0,601	3259,068	62,877	151,664
NS E7	102,788	1,806	95,445	0,879	8995,112	28,245	51,088
NS E6	91,916	1,544	85,350	0,617	123,604	2,451	5,652
NS E5	87,126	1,528	80,903	0,601	1019,067	5,079	11,391
NS L4	93,997	0,911	87,283	0,601	2179,274	29,476	71,327
NS D2	83,340	1,862	77,387	0,601	596,382	7,449	15,982
NS B1	90,095	1,912	83,659	0,634	454,952	7,152	15,716

Table A.6: Reliability indices for every delivery point - Scenario 3

Description	Demand [kW]	Reference Demand [kW]	Agriculture	Residental	Industry	Commercial	Public sector	Large industry
NS M3	17,75171233	40,63702774	0	0,356978875	0	0	0,643021125	0
NS M4	14,62968037	31,02181435	0	1	0	0	0	0
NS L3	100,0430365	207,7600708	0,055982756	0,87550221	0,004375971	0,064139063	0	0
NS L5	52,77134703	111,9026108	0	1	0	0	0	0
NS L4	49,03139269	100,0848694	0	0,910110241	0	0,089889759	0	0
NS I3	0	1,29E-19	0	1	0	0	0	0
NS I1	90,82340183	185,7659607	0,049064055	0,569966805	0,005821926	0,199282817	0,175864396	0
NS H6	37,9890411	75,15598297	0,280220804	0,443134285	0,026632891	0,25001202	0	0
NS I2	46,71335616	96,97972107	0	0,955531281	0	0,029681654	0,014787065	0
NS L1	16,79977169	33,60718918	0	0,870588315	0,129411685	0	0	0
NS K2	17,53447489	37,18190765	0	1	0	0	0	0
NS H5	21,97100457	41,23941422	0,106236946	0,301216838	0,592546216	0	0	0
NS K3	27,81723744	58,58832169	0	0,983769631	0	0,016230369	0	0
NS K1	29,95445205	73,86491299	0	0,195151695	0	0	0,804848305	0
NS J3	10,10673516	22,16385269	0	0,488801039	0	0,511198961	0	0
NS H4	41,7456621	85,15949249	0,062651083	0,867888824	0	0,04855999	0,020900102	0
NS H2	27,67134703	58,67710876	0	1	0	0	0	0
NS J2	13,04166667	25,99019623	0,414311348	0,585688652	0	0	0	0
NS J1	15,59531963	32,56358719	0	0,963151923	0	0,036848077	0	0
NS H1	876,4333296	4269,108795	0	0	0	0,989254913	0,010745087	0
NS E6	3,973059361	8,421066284	0,003275486	0,996724514	0	0	0	0
NS E7	32,11552511	81,88329315	0	0	0	1	0	0
NS E5	8,44783105	21,53918457	0	0	0	0	1	0
NS G2	43,74577626	94,69120026	0,202683625	0,797316375	0	0	0	0
NS F4	0,000684932	0,002023273	0	0	0	0	1	0
NS F5	29,74931507	75,85018158	0	0	0	0	1	0
NS E4	159,3059361	406,17276	0	0	0	0	1	0
NS F3	12,39006849	31,59022331	0	0	0	1	0	0
NS F2	1,537442922	3,920008659	0	0	0	0	1	0
NS E3	0	1,29E-19	0	1	0	0	0	0
NS F1	0,849429224	1,872278571	0	0,474129821	0	0,335438785	0,190431394	0
NS E1	92,46575342	2,910547495	0	0	0	0,012345679	0,987654321	0
NS E2	39,64166667	51,2024765	0	0	0,939169674	0,060830326	0	0
NS C3	63,41084475	126,1433716	0	0,647113572	0	0,345890664	0,006995764	0
NS C1	463,7446347	897,0055542	1	0	0	0	0	0
NS C2	301,8889269	584,0177612	0,968273205	0,031726795	0	0	0	0
NS D2	12,39098174	25,3226757	0	0,704979502	0	0	0,295020498	0
NS B2	21,68561644	41,47318268	0,192065949	0,544971205	0,262962846	0	0	0
NS B1	11,27146119	21,82330704	0,787103243	0,212896757	0	0	0	0
NS D1	62,83116438	130,117981	0,038669988	0,918579363	0	0	0,042750649	0
NS A2	25,66347032	52,89866638	0,192418554	0,807581446	0	0	0	0
NS A1	0,924885845	1,789134026	1	0	0	0	0	0
NS M2	21,39109589	48,37008286	0	0,395285667	0	0,107857577	0,496856756	0
NS M1	40,02340183	79,51446533	0	0,812909114	0	0,187090886	0	0
NS L2	104,5926941	220,9541626	0	0,990938976	0	0	0,009061024	0
NS H3	40,32899543	81,27321625	0,04043512	0,874711986	0,064517864	0	0,02033503	0
NS G1	9,167123288	23,37313652	0	0	0	1	0	0

Table A.7: Input parameters for every delivery points in the grid

Hour	**Energy Consumption [MWh/h]**
1	1,427
2	0,856
3	0,587
4	0,844
5	0,848
6	2,496
7	5,470
8	5,800
9	5,968
10	6,712
11	7,994
12	9,811
13	10,000
14	10,000
15	10,000
16	10,000
17	10,000
18	10,000
19	10,000
20	10,000
21	10,000
22	6,402
23	3,867
24	2,633

Table A.8: Energy consumption at fast charging station - June 29

Hour	CENS [NOK/hour]	ENS [kWh/hour]	Interrupted power [kWh/hour]
1	59,9088	0,6140	0,2886
2	59,8213	0,5293	0,2494
3	59,7240	0,4893	0,2309
4	59,8182	0,5275	0,2486
5	59,8193	0,5281	0,2489
6	59,9664	0,7727	0,3620
7	60,0089	1,2142	0,5661
8	60,0110	1,2631	0,5887
9	60,0119	1,2882	0,6003
10	60,0156	1,3985	0,6513
11	60,0203	1,5889	0,7393
12	60,0249	1,8585	0,8640
13	60,0253	1,8866	0,8769
14	60,0253	1,8865	0,8769
15	60,0253	1,8865	0,8769
16	60,0253	1,8865	0,8769
17	60,0253	1,8865	0,8769
18	60,0253	1,8865	0,8769
19	60,0253	1,8865	0,8769
20	60,0253	1,8865	0,8769
21	60,0253	1,8865	0,8769
22	60,0142	1,3525	0,6300
23	59,9941	0,9761	0,4560
24	59,9704	0,7930	0,3713

Table A.9: Reliability indices per hour for worst case scenario

Marte Røine Bruråsen

Impact of Fast Charging Stations on the Reliability of Electricity Supply in Distribution Networks

NTNU
Norwegian University of
Science and Technology